FACILE FABRICATION OF NANOCELLULOSE BASED AEROGEL FOR REMOVAL OF HEAVY METAL IONS FROM WASTE WATER

Thesis submitted towards the partial fulfilment of Masters of Engineering degree in Chemical Engineering

by

AVRA MONDAL

Exam Roll No: M4CHE24005

Class Roll No.: 002210302005

Registration No.: 143962

Session: 2022 – 2024

Under the guidance of

Dr. Sudeshna Saha

Prof. Sushanta Mitra

DEPARTMENT OF CHEMICAL ENGINEERING

JADAVPUR UNIVERSITY

Kolkata - 700032

DECLARATION OF ORIGINALITY AND COMPLIANCE OF ACADEMIC ETHICS

I hereby declare that this thesis contains literature survey and original research work by the undersigned candidate, as part of his "***Master of Engineering in Chemical Engineering***" studies. All information in this document have been obtained and presented in accordance with academic rules and ethical conduct.

I also declare that, as required by these rules and conduct, I have fully cited and referenced all material and results that are not original to research work.

Name: **AVRA MONDAL**

Registration No.: 139462

Thesis Title: Facile fabrication of nanocellulose based aerogel for removal of heavy metal ions from waste water

Signature:

Date:

CERTIFICATION

This is to certify that **Mr. Avra Mondal**, final year student in Master of Chemical Engineering examination in the Department of Chemical Engineering, Jadavpur University, bearing Registration No: 143962 has successfully completed the thesis work entitled **"Facile Fabrication of Nanocellulose Based Aerogel for Removal of Heavy Metal Ions from Waste Water"** under the guidance of **Dr. Sudeshna Saha and Prof. Sushanta Mitra** during his master degree curriculum. This work has not been reported earlier anywhere and can be approved for submission in partial fulfilment of the requirements for the Master of Engineering in Chemical Engineering.

Assistant Professor
CHEMICAL ENGINEERING DEPARTMENT
JADAVPUR UNIVERSITY
Kolkata-700 032

Sudeshna Saha. 30/8/24

Dr. Sudeshna Saha
Project Supervisor
Chemical Engineering Department
Engineering
Jadavpur University
Canada

Prof. Sushanta Mitra
Project co-supervisor
Mechanical & Mechatronics
University of Waterloo,

Ratna Dutta 30/08/24

Dr. Papita Das
Head of the Department
Technology
Chemical Engineering Department
Jadavpur University

HEAD (offg.)
CHEMICAL ENGINEERING DEPARTMENT
JADAVPUR UNIVERSITY
Kolkata-700 032

Dipak Laha 30.8.24

Prof. Dipak Laha
Dean
Faculty of Engineering &
Jadavpur University

DEAN
Faculty of Engineering & Technology
JADAVPUR UNIVERSITY
KOLKATA-700 032

CERTIFICATE OF APPROVAL

This thesis is hereby approved as creditable study of an engineering subject carried out and presented in a manner satisfactory to warrant its acceptance as prerequisite to the degree for which it has been submitted. It is understood by this approval that undersigned don’t endorse or approve any statement made, opinion expressed or conclusion drawn therein but approve the thesis only for purpose of which it is submitted.

.....

Avra Mondal

Department of Chemical Engineering

Jadavpur University

ACKNOWLEDGEMENT

Though the following project is individual project work, but I would have never been successful in completing my work in a smooth manner without help, guidance, assistance, and inspiration from a lot of people. At the start of this report, I would like to thank all those persons who have helped me in this endeavor. Without their guidance and help it would not be possible for me to progress and plan about this project.

I would sincerely express my gratitude towards my project guides Dr. Sudeshna Saha and Dr. Susanta Kumar Mitra for their valuable guidance and cooperation and for providing me the opportunity to accomplish the project. Without their guidance and assistance, I would never be able to work successfully in this area. I am greatly thankful to them for guiding me always throughout my project work.

I would like to thank all my lab mates who consistently helped me while performing and planning this project.

I would also like to express gratitude to HOD and all faculties of the Chemical Engineering Department, Jadavpur University.

Thanking you,
Avra Mondal
Class Roll Number – 001710302005
Registration Number – 143962 of 2022-24
M.E. 2nd Year

Table of Content

1. Introduction……1

1.1. Water pollution……1

1.2. Sources, effects and regulations on heavy metal water pollution……..2

1.2.1. Sources of heavy metal and metalloid pollution……2

1.2.2. Toxicological effects of heavy metals and metalloids……3

1.3. Removal of heavy metals from water……5

1.3.1. Factors affecting heavy metal removal……..6

1.3.1.1. Effect of pH……6

1.3.1.2. Effect of temperature……..6

1.3.1.3. Effect of ionic strength……...7

1.3.1.4. Effect of natural organic matter……..7

1.3.2. Mechanisms for the removal of heavy metal and metalloid ions…...8

1.3.3. Conventional treatments……9

1.3.3.1. Chemical precipitation……9

1.3.3.2. Coagulation/flocculation……9

1.3.3.3. Ion exchange ……..…9

1.3.3.4. Membrane technologies……..……..10

1.3.3.5. Electrochemical technologies……...10

1.3.4. non-conventional treatments…….……11

1.3.4.1. Adsorption……11

1.3.4.2. Activated carbon ……..……12

1.3.4.3. Polymeric materials…….……12

1.3.4.4. Agricultural residues……..……...12

1.3.4.5. Industrial wastes…….……..13

1.3.4.6. Magnetic adsorbents……..……...13

1.3.4.7. Composite adsorbents……..……13

1.3.4.8. . Microbial fuel cell……...14
1.3.4.9. Nanotechnology……...14
1.3.4.10. Nanocarbon (carbon nanotubes, graphene and other carbon derivatives)…….. …….15
1.3.4.11. 2D materials……16
1.3.4.12. Nanoparticles……...16
1.3.4.13. Commercial products for heavy metal removal ……...17
1.3.4.14. Fenton-like reactions ……...17
1.3.4.15. Plant-mediated remediation of heavy metals……18
2. Literature review……21
2.1. literature review on Sol-Gel method…….21
2.1.1. Sol–gel-based aerogel synthesis……...21
2.1.2. Sol preparation……..……21
2.1.3. Gel formation……..……..21
2.1.4. Aging……..……..21
2.2. literature review for drying methods…….21
2.2.1. Drying…….……..21
2.2.1.1. Ambient pressure drying……21
2.2.1.2. Freeze-drying (lyophilizer) process…….…..……22
2.2.1.3. Supercritical drying……24
2.3. Comparison between various drying methods……..……24
2.4. Literature Review of CNC based aerogel for heavy metal ion removal…….……25
2.5. Aims and Objectives …….……...30
2.5.1. Aim……...30
2.5.2. Objective……...30
3. Experimental Methods ……..……32
3.1. Experimental Design ……..……..32

3.2. Materials & methods…….32

3.2.1. Fabrication of nano cellulose aerogel……..….32

3.2.2. Characterization of prepared Aerogels…….34

3.3. Batch adsorption Experiment of Cu……..34

3.3.1. Batch Adsorption Experiment of Cr(VI)……..34

3.3.2. Adsorption Studies of Heavy Metals……35

3.3.3. Heavy metal concentration determination using ICP-OES……..35

4. INSTRUMENTS AND APPARATUS…….……..36

4.1. BET Surface Area Analyzer …….……36

4.2. Thermogravimetric analyzer…….……38

4.3. FTIR (Fourier-Transform Infrared Spectroscopy…….40

4.4. Inductively Coupled Plasma Optical Emission Spectroscopy (ICP-OES)……..42

5. Novelty of Work……44

6. Results……..…..45

6.1. Removal of Cr (VI) ion using surface modified aerogels…….45

6.2. Removal of Cu (II) ion using surface modified aerogels…….....45

6.3. Effect of pH…….……..46

6.3.1. Effect of pH in Cu (II) adsorption…….……46

6.3.2. Effect of pH in Cr (VI) adsorption…….47

6.4. Effect of adsorbent dosage ……...47

6.4.1. Effect of adsorbent dosage for Cr(VI)adsorption……48

6.4.2. Effect of adsorbent dosage for Cu (II)adsorption…….……48

6.5. FTIR analysis……49

6.6. Adsorption kinetics……..…….52

6.7. Adsorption isotherms……..……...57
6.8. BET analysis…….61
6.9. TGA analysis……..……..63
7. Conclusion…….…….…….…….……64
8. REFERENCE…….……66

List of figures:

Figure 1: Experimental design……..…….……32
Figure 2: BET by Quantachrome Autosorb……36
Figure 3: TGA by PerkinElmer……..38
Figure 4: FT/IR-4700 by JASCO……40
Figure 5: ICP by PerkinElmer…….42
Figure 6: Removal of Cr……45
Figure 7: Removal of Cu…….……45
Figure 8: pH variation for Cu…….46
Figure9: pH variation for Cr…….……..47
Figure 10: Dosage variance for Cr……..……48
Figure11: Dosage variance for Cu…….…….49
Figure 12: FTIR of Aerogels……..…….……49
Figure 13: Cr adsorption…….……50
Figure 14: Cu adsorption…….……...51
Figure 15: Kinetics Data …….…….……..52
Figure 16: 10ppm kinetic data for pseudo 1st order……53
Figure 17: 10ppm kinetic data for pseudo 2nd order……54
Figure 18: 100ppm kinetic data for pseudo 1st order……..55
Figure 19: 100ppm kinetic data for pseudo 2nd order…….55
Figure 20: 200ppm kinetic data for pseudo 1st order……..55
Figure 21: 200ppm kinetic data for pseudo 2nd order…….55

Figure 22: 1000ppm kinetic data for pseudo 1st order…….56
Figure 23: 1000ppm kinetic data for pseudo 2nd order……56
Figure 24: Langmuir Isotherm……58
Figure25: Freundlich Isotherm…….…….…….……58
Figure 26: DR Isotherm……..…….…….……..59
Figure27: Temkin Isotherm……..…….…….……60
Figure 28: S4 BET isotherm…….…….…….……...61
Figure 29: S6 BET isotherm……..62
Figure 30: S4 TGA……..…….…….……63

List of Tables:

Table 1: Source of contamination……....4
Table 2: Drying method comparison…….…….…24
Table 3: Literature review……..25
Table 4: Sample components……..……...33
Table 5: kinetics data…….53

1. Introduction

1.1.Water pollution

Water is the most essential component for life in earth and access to clean water has become one of the greatest concerns of modern time. Increase in population, rapid urbanization, unplanned industrialization and careless utilization of natural resources has caused severe damage to the quality of water. Organic matter, nutrients, pharmaceutical and personal care products, poly- and perfluoroalkyl substances, biocides, heavy metals, dyes, radionuclides, plastics, nanoparticles and pathogens are among the pollutants of major concern. Heavy metal ions are among the most released contaminants, and for this reason they are particularly worrisome. Heavy metals and metalloids are elements presenting an atomic density greater than 4 g/cm3; therefore, they include copper (Cu), cadmium (Cd), zinc (Zn), lead (Pb), mercury (Hg), arsenic (As), silver (Ag), chromium (Cr), iron (Fe) and platinum (Pt) group elements. These metallic toxic elements are daily released into the water from diverse natural and anthropogenic sources. In several places around the world, the average concentrations of Cr, Mn, Fe, Co, Ni, As, and Cd found in surface water bodies are well above the maximum allowed values for drinking water. This represents a public concern. Heavy metals are not biodegradable; therefore, they tend to bioaccumulate, which is their overtime increase of concentration in living organisms. They are also persistent and can directly or indirectly affect various organisms due to biomagnification. Many heavy metal ions are toxic or carcinogenic. Even at very low concentrations they can induce multiple organ damage affecting lungs, kidneys, liver, prostate, esophagus, stomach and skin, and can also cause neurodegenerative disorders and diseases, such as Alzheimer and Parkinson diseases. Metals can also affect aquatic organisms (phytoplankton, zooplankton, and fish), accumulating in several organs and causing oxidative damage, endocrine disruption, and depression of the immune system, which can also affect survival and growth. These effects, as well as the potential ecological impacts of heavy metals, require the development of technologies to efficiently remove them from water.

Multiple approaches have been developed for removing heavy metals from water. Conventional treatments (e.g. chemical precipitation, ion exchange, and electrochemical removal) show many disadvantages including incomplete removal, high-energy requirements, and production of toxic sludge. Additional difficulties could be associated with the capital and technical requirements for installation, operation, and maintenance, which can result in an inadequate application of these technologies, particularly in decentralized contexts and developing countries. Thus, there is a need to develop effective and environmentally friendly solutions, which

include, for instance, adsorption methods by using biopolymers, biological, or nanotechnology approaches.

1.2 Sources, effects and regulations on heavy metal water pollution

1.2.1 Sources of heavy metal and metalloid pollution

Approximately 40% of the lakes and rivers of the planet have been polluted by heavy metals. The sources of these pollutants can be natural and anthropogenic. Natural sources include the interactions with metal containing rocks, normally present in the environment, and volcanic eruptions. The contribution of volcanoes can occur due to large but sporadic emissions, explosive volcanic activity, or continuous low emissions, including geothermal activity and degassing. Anthropogenic sources include those associated with industrial (e.g., fossil fuel combustion, metal processing), agricultural (pesticides) and domestic activities (e.g. garbage, detergents). Mining is one of the key sectors to be considered, particularly because it plays a central role in the economies of developed and developing countries. This activity generates a large presence of heavy metals, released due to the extraction of minerals, and transported through rivers and streams, in which they can be dissolved in water or as part of sediments. These metal species tend to seep into groundwater, and can also cause water scarcity, prevent the growth of crops due to soil erosion, and bring serious health problems on animals and local human communities.

Anthropogenic activities, urbanization, and industrialization represent key factors in increasing the concentration of these pollutants, particularly in recent decades. In India, it was reported that the concentration of arsenic reached 107 g/L in drinking water. Contamination of heavy metals in India has been observed across the nation. Nearly 718 districts have contaminated groundwater with arsenic, cadmium, chromium, and lead. Arsenic-contaminated groundwater covers major states such as Bihar, West Bengal, Uttar Pradesh, Jharkhand, Assam, Manipur, and Chhattisgarh (WHO 2019). On the other hand, polluted air and crop fields have also been reported, especially selenium toxicity, in 9% of people in Hoshiarpur and Nawansahar districts of Punjab (Jamwal 2015). Industrialization is one of the major contributors of contamination to sites like Vadodara (Gujarat), Ranipet (Tamil Nadu), Talcher (Orissa), Ratlam (Madhya Pradesh), Ganjam (Orissa), Singrauli (Madhya Pradesh), Balai (Uttar Pradesh) and Malanjkhand (Madhya Pradesh). Ganga, the national river of India, is polluted with chromium, copper, nickel, lead, and iron. The Ministry of Environment, Forest and Climate Change (MoEF&CC) has identified 320 locations of high probability of contamination with heavy metals (Cr, Pb, Hg, As, and Cu) and pesticides in India, Moreover, around 140 million people in 50 countries regularly drink water that contains arsenic with concentrations higher than the WHO reference value of 10 g/L .Given the magnitude of the pollution problem, developing and developed countries must find a way to rapidly reduce the

concentration of heavy metals in water environments and to avoid the potential effects on human health. For developing countries, one of the main limitations is a low economic capacity to develop and apply remediation technologies.

1.2.2 Toxicological effects of heavy metals and metalloids

Heavy metals accumulate in their given chemical form or in combination with other metals, making it difficult to remove them from water .Trace quantities of these metals (e.g. Co, Cu, Cr, Fe, Mg, Mn, Mo, Ni, and Zn), are necessary for metabolic activities, to avoid diseases and syndromes in humans .However, an excess concentration of these same heavy metals can lead to serious human health problems such as muscular, physical and neurological degenerative processes .Long exposure periods to toxic heavy metals have been associated with muscular dystrophy, Alzheimer's disease, different types of cancer and multiple sclerosis. Damaged or decreased central nervous and mental activities, damage to the lungs, liver, kidneys, blood compositions, and other key organs have also been observed. The discharge of heavy metals into water sources can also lead to physical, chemical, and biological disorders, generating changes in diversity, density, species composition of population, and structure of the community. The nature and degree of change will largely depend on the heavy metal ion concentration, and may even interrupt enzymatic processes.

1.2.3 Policies and regulations for the presence of heavy metals in water

Several environmental regulations define cleanliness criteria and maximum permissible limits for different polluting compounds and/or materials in water. These limits depend on factors such as: physical characteristics of the affected area, properties of the polluting compound or material, associated environmental regulations, infrastructure, human resources and available technologies. In the case of heavy metals, there are specific regulations that allow controlling their maximum permitted concentration. Besides, there also exist standards where environmental safety criteria are established for various types of pollutants in different ecosystems. In some countries, it is also recurrent to use foreign standards on environmental protection as a legal reference framework. This framework is accompanied by cross-disciplinary and multi-stakeholder committees for the further discussion and analysis. Depending on the region, geographically close standards are often used. For example, in the American continent, it is very common to use the USEPA environmental regulations. In Europe it is well known the European Environment Agency (EEA), which grouping indicators, data, publications and some common regulations are used among the member countries.

Table 1: Source of contamination

Heavy metal	Anthropogenic source	Maximum concentration level µ g L^{-1}	toxicity		Adverse effect on health	References
			Tolerable daily intake(mg/day)	Lethal dosage (mg/kg Body Weight)		
Lead	• Metal purifying • Pesticides • Vehicular • Fertilizers • Coal • gasoline	10	0.025-0.052	94-158	Kidney and nervous system damage, mental retardation and cancer to human body	WHO(2017)
Cadmium	• Electroplating • Metallurgical industry • Petroleum • Insecticides • Synthetic chemicals	3	0.018-0.052	4.4-6.2	Hepatic toxicity, lung cancer, Kidney liver, Reproductive organs disorder	WHO(2017)
Mercury	• Fossil fuel combustions • Electronic industries • Plastic industris • Paper and pulp industries	6	0.03	5.1-10	Damage to kidney, liver, Respiratory system	WHO(2017)
Zinc	• Minning • Coal combustion • Industrial • electroplating		15-20	16.1-25.3	Pain, skin inflation, vomiting, anemia	WHO (2017)
Nickel	• Pulp and paper mills • Fertilizers • Petroleum refineries • Electroplating • Battery • metal alloys industry	70	.089-.231	NA	Dry cough,nausea, Cheast pain, Pulmonary fibrosis,Breathing problem	WHO (2017)
Chromium	• industries • Textile industry • Electroplating • anti corrosive product	50	.013-.099	NA	Skin diseases, Inflammatory diseases, Vomiting	WHO (2017)

	• Industrial wastage • Tanning industry					
Copper	• Minning industry • Metallurgy • Chemical industries • Steel Industries • Electroplating Industries	2000	10	4-7.2	Hair loss, Anemea, Kidney disorder	WHO (2017)
Arsenic	• Industrial waste water • Fly ash • Irrigation with municipal water • Composts • Electronic production • Livestock manures	10	.03	41	Skin damage, Cancer, Circulatory diseases	WHO (2017)

1.3 Removal of heavy metals from water

Wastewater treatment technologies can be classified in primary, secondary, and tertiary treatments. Primary treatment focuses on the removal of organic matter and suspended solids from wastewater through physical and chemical processes. Microfiltration, chemical filtration, coagulation, and flocculation are the important primary technologies when dealing with high concentrations of heavy metals. Secondary treatments (anaerobic or aerobic) are based on natural microorganisms capable of converting organic and inorganic contaminants into simpler and safer substances, which allow higher removal efficiency. The microbial effectiveness to eliminate metals is still under study, but results have shown high removal rates. Tertiary treatments include chemical oxidation, electrochemical precipitation, crystallization, distillation and photocatalysis, adsorption, membrane technologies, and ion exchange technologies. In this stage, wastewater is converted into good quality water. Removal efficiencies that reach up to 99% can be obtained when tertiary treatments are adequately combined with primary and secondary treatments.

1.3.1 Factors affecting heavy metal removal

Each metal has different properties and behaviors; thus, we must analyze the parameters that influence their removal from water. The next sections summarize the influence of pH, ionic strength, temperature, and natural organic matter content, on the heavy metal elimination from domestic wastewater effluents, groundwater, rivers, and lakes.

1.3.1.1. Effect of pH

Changes in pH can alter the balance of organic and inorganic substances found in water, affecting the removal of the present contaminants. These changes can be produced by the chemicals added during the remediation treatment or may originate in biological instabilities. At neutral pH values or lower, heavy metals are in the cationic state and tend to be more soluble and mobile in water. On the other hand, higher pH values affect their oxidation state and promote the formation of hydroxides and other anions. For instance, the removal efficiency and adsorption capacity of a natural clay used to remove Ni^{2+} depends on the pH of the solution. As the pH increased, the nickel removal efficiency also increased.

1.3.1.2.Effect of temperature

Tests carried out with different types of treatments show that there is a greater removal effectiveness when the temperature is higher. For example, the efficiency of Cd^{2+}, Cu^{2+}, $Pb^{2+}$and Ni^{2+} removal by using plants increased when the temperature reached the maximum level at 55 °C. The variation of the adsorption capacity of Cu^{2+} and Pb^{2+} on hydrogels was investigated at different temperatures (22, 30, 35, and 40° C). The maximum capacity was reached at 30 C for Pb^{2+} and 35 °C for $Cu^{2+.}$ An increase up to 40° C increased slightly the removal outcome. The efficiency of removing Cr^{6+} using pistachio residues improved when the temperature went from 5 to 40° C. This was explained by the increase of adsorption sites on the surface of the residues. Moreover, in a work performed using biomass from fungi, the biosorption efficiency of heavy metals increased when the temperature was raised from 10° C to 60° C. This was explained by a higher affinity of the active sites of the biomass substrates.

On the other hand, slight temperature increases can also affect negatively the heavy metal removal. For instance, a temperature increase reduced the removal efficiency ofNi2+, Cu2+, and AJ3+ when magnetic iron oxide nanoparticles were used as adsorbents. This is because at higher temperatures the rate of chemisorption did not allow the heavy metals to reach new active sites on the nanoparticle surface to improve the metal removal. Also, the temperature can change the size of the nanoparticle pores resulting in a lower adsorption.

1.3.1.3.Effect of ionic strength

The ionic strength is given by the total concentration of ions in the aqueous solution, as well as their chemical charge. This strength influences the ion exchange mechanism between heavy metal ions and adsorbents, and the ability to remove heavy metals. For instance, the adsorption of $Cr^{3+,}$ $Pb^{2+,}$ zn^{2+} and Cu^{2+} ions on a porous magnetic material slightly decreased when the concentration of NaCl increased. In another study, the sorption of Cu^{2+} and Ni^{2+} on bentonite increases with decreasing ionic strength at pH 5.5, reaching a maximum adsorption at NaCl concentrations lower than 0.05 M. This is because a higher ionic strength can reduce the electrostatic repulsion of the molecules, increasing the aggregation of particles, which reduces the amount of available binding sites in the system and decreases the sorption. Additionally, the presence of chloride can promote the formation of soluble heavy metal chloride complexes that are difficult to remove from water. This is because the chloride complexes formed have low adsorption affinity.

1.3.1.4. Effect of natural organic matter

Natural organic matter (NOM) is present in the water sources, and particularly in surface waters, due to the interactions with the biosphere and geosphere (e.g. decomposition of animals and plants in water). As a result, NOM can interact with heavy metal water pollutants through mechanisms such as ion exchange, chelation, and adsorption. Even though it is impossible to exactly determine the influence on the removal of heavy metals, the presence of NOM affects their reactivity, mobility, bioavailability and toxicity. For instance, lead can form complexes with NOM present in natural waters or wastewater, making it more mobile and difficult to eliminate using conventional processes such as chemical precipitation, coagulation/flocculation. A study conducted with titanate nanotubes supported on powder activated charcoal showed that the capacity of adsorption of Pb^{2+} is influenced by the formation of complexes and weak interactions between nanotubes and dissolved organic matter. Large amounts of NOM could also hinder the absorption and removal of heavy metals due to ionic competition, complex formation, and simultaneous chelation between metals and NOM.

These factors and their combinations are significant challenges for the removal of heavy metals from water and may affect the reproducibility which should be taken into account when testing removal methods.

1.3.2. Mechanisms for the removal of heavy metal and metalloid ions

Understanding the interaction mechanisms that allow the removal of heavy metal and metalloid ions from solutions is still an open issue. Most of the modern remediation methodologies involve somehow either the sorption, sorption-reduction and/or the photocatalytic degradation. In this context, the determination of the physicochemical properties of these pollutants, and the combination of advanced characterization (e.g. spectroscopy measurements) with theoretical calculations at molecular level seems to be mandatory to understand their potential impact in the natural environment and to define alternative elimination routes .One of the simplest mechanisms for the uptake of heavy metal and metalloid ions from solutions is found on the sorption due to chemical interactions between functional groups (particularly those with different oxygen-containing groups, hydroxyl groups or carbonyl groups) and metal ions. Such mechanism is governed by the formation of strong surface complexes through hydrophobic interactions, n-n donor-acceptor interactions, hydrogen bond interactions and/or electrostatic attraction. Likewise, the sorption-reduction represents another mechanism for the immobilization and reduction of high valent metal ions to low valent metal ions. In this process, the high valent metal ions are first reduced and then they form more dense particles or clusters which easily precipitate. Typical examples of such sorption-reduction mechanisms would be Cr^{6+} to $Cr^{3+,}$ Se^{4+} to Se^{2+} among others. Thus, the low valent metal ions are much more biofriendly in the natural environment. It is widely accepted that this mechanism is governed by the fact that high valent metal ions are much more mobile whereas the low valent metal ions are less mobile. Finally, the photocatalytic degradation mechanism under visible light irradiation is often used to remove other organic contaminants such as persistent organic pollutants (POPs); however, it has been used widely for the removal of low concentrated heavy metal and metalloid ions from solutions .This strategy is based on the photocatalytic reactions, which depend on the morphologies of the catalyst, mass transport processes, visible-light absorption and surface distribution of active sites .As reported in the literature, a very common route is to produce tailored nanoparticles or composites in which the energy gap can be controlled to improve the photocatalytic efficiency . It is worth mentioning that radionuclide ions can also be efficiently removed from aqueous solutions by taking advantage of the sorption or sorption-reduction strategies. Radionuclide pollution became an extremely important environmental issue during the last century, mainly due to the fact that some radionuclides have half-lives of a fraction of a second, but others have half-lives of millions of years. By definition, radioactive forms of elements are called radionuclides. Some of them, occur naturally in the environment, while many others are fabricated, either deliberately or as byproducts of nuclear reactions. Some

examples of the most common radionuclide pollutant found in water would be uranium, U^{6+} ions, dissolved in water as a complex anion ($UO_2(CO_3h]^{4-}$ and technetium-99 (99Tc) dissolved in the environment in the +7-valence state in the form of pertechnetate anion $(TcO_4)^-$. The main sources for such pollutants in hydric sources include the active production of nuclear power, the rapid development of nuclear power plants and the mining activities and extraction of uranium.

1.3.3. Conventional treatments

This section describes some conventional methods for removing heavy metals from wastewater and their fundamental principles. Their advantages and disadvantages are also presented.

1.3.3.1.Chemical precipitation

Chemical precipitation is an effective technique used to remove heavy metals, mainly from the discharges of the paper production and electroplating industries. In this process, chemical precipitants such as alum, lime, iron salts, and some polymers react with heavy metals present in wastewater, resulting into insoluble precipitates. Through this reaction, metals can be removed more easily. The removal capacity and efficiency can be improved by optimizing parameters such as pH, temperature, initial concentration.

1.3.3.2. Coagulation/flocculation

Coagulation-flocculation is a highly efficient physicochemical method for removing heavy metals. In this process, fine particles and colloids agglomerate into larger particles, which reduces turbidity, NOM, and other wastewater pollutants. In the first stage, a coagulant added to water stimulates the coalescence of colloidal material into small aggregates known as floes. Among the most widely used coagulants are aluminum sulfate, ferric sulfate, polyaluminum chloride (PACI), polymeric ferric sulfate (PFS) and polyacrylamide (PAM) In the second stage, the floes agglomerate under gentle agitation, settle, and then are disposed of as sludge. This process is used as a pre-treatment, post-treatment, or main wastewater treatment due to its versatility.

1.3.3.3. Ion exchange

In this process, a reversible ion exchange occurs between solid and liquid phases. Particularly, an insoluble substance removes the ions from an electrolytic solution and releases other ions of a similar charge in a chemically equivalent amount. The most common ion exchange materials are synthetic organic resins in organic three-dimensional matrix, and new generation hybrid materials. Using an adequate ion

exchange resin can provide an effective and economical solution to contamination control requirements. In the case of heavy metals, after separating the loaded resin, more concentrated metals are recovered by elution with suitable reagents. The resin with acid functional groups contains sulfonic acid in its structure. where RSO_3 and Mo^+ represent the anionic group attached to the ion exchange resin and the metal cation, respectively, while n is the coefficient of the reaction component and depends on the oxidation state of the metal ions.

1.3.3.4. Membrane technologies

A membrane is a barrier that allows the passage of a selected set of compounds while blocking the passage of others. This technology is governed by the size exclusion or steric hindrance mechanism, the Donnan exclusion effect (charge-charge repulsion), and the adsorption capacity of specific contaminants This type of treatment can be used to remove suspended solids, organic and inorganic contaminants .Depending on the material used to manufacture them, membranes are classified as organic (made of synthetic organic polymers, such as polyethylene or cellulose acetate) or inorganic (made of ceramics, metals, zeolites, silica, among others) .

Membrane processes can be classified according to their driving force: driven by low pressure (microfiltration (MF), ultrafiltration (UF), distillation), driven by high pressure (nanofiltration (NF) and reverse osmosis), and by osmotic pressure (e.g., direct osmosis (FO), electrodialysis (ED) and liquid membrane (LM)). MF, UF, NF and reverse osmosis (RO) are the main methods used in the removal of heavy metals from wastewater. Factors such as the size and distribution of the pores, the surface charge, the degree of hydrophilicity, the flow of the solution, and the presence of functional groups, must be considered because they significantly affect the removal performance of a membrane .As an example, RO membranes can remove up to 99% of metal and metalloid ions such as As+, cu2+ or Cd2+, and can be used not only with wastewaters but also with other types of water, such as groundwater. Nanocomposite membranes can also achieve high removal rates (80%-98%) when working with synthetic water containing metal and metalloid pollutants such as arsenic, chromium, cadmium, lead, and zinc.

1.3.3.5. Electrochemical technologies

Electrochemical treatment methods are effective in removing heavy metal ions from water sources. These methods involve the recovery of metals in their elemental metal state, by using anodic and cathodic reactions in an electrochemical cell. Electrochemical treatments include electrodeposition, electrocoagulation, and electro flotation. Electrocoagulation originates from conventional chemical

coagulation. In this process, a set of electrodes act as anode and cathode where oxidation and reduction reactions take place. The charged ionic metals react with the anion in the effluent and the coagulant is generated by electrolytic oxidation of a suitable anode material. The simultaneous cathodic reaction allows the removal of contaminants either by deposition on the cathode or flotation. This process is easy to operate, does not require chemicals, and has a reduced sludge production.

Electrodeposition is extensively used for the recovery of toxic metal ions (e.g., Pb, Cd, Cu, Ni, Zn or Cr) from industrial wastewaters or to recover precious metals (e.g., Ag, Pt, Au, etc.) from solutions. The electrochemical mechanism for metal recovery is based on cathodic reduction. The main advantages of this method include simple equipment, easy and low cost of operation. Electro flotation is based on the solid-liquid separation that allows the metals to float on the surface of water through small bubbles of oxygen and hydrogen gases, a reaction that occurs through the electrolysis of water. The bubbles adhering to the pollutants and the resulting pollutant-bubble complexes move up to the liquid surface where foam can be periodically skimmed off. This process can be used to remove metals from wastewater, including Pb2+, cu2+, Ni2+, zn2+, and Fe3+. Electrochemical techniques are environmentally compatible, versatile, energy efficient, safe, selective, amenable to automation and cost effective.

While the development of the membrane technologies keeps improving with new materials and at lower cost, the electrochemical technique remains very practical and efficient among the conventional treatment methods.

1.3.4. non-conventional treatments

This section describes the main advanced and more recently developed treatment methods, including adsorption, microbial fuel cells, nanotechnology, and Fenton like reactions.

1.3.4.1. Adsorption

Adsorption is among the best methods to remove a wide variety of contaminants from water, including heavy metals. Among its advantages we can highlight a high removal capacity, relatively low energy consumption and technical requirements for operation, and the possibility of avoiding major secondary pollution Adsorbents should have a series of desirable properties, such as a large specific surface area, high mechanical strength, good thermal stability, controllable morphology environmentally friendly nature and processing. This should translate into a high performance, given by high adsorption capacity and efficiency, selectivity, low-cost, and reusability. Activated carbon (AC), polymer-based materials,

biomaterials, magnetic materials, agricultural and industrial residues are some of the most used adsorbents.

1.3.4.2. Activated carbon

AC is the most used heavy metal adsorbent, and can be obtained by the pyrolysis/carbonization of a wide range of carbon-containing materials, followed by an activation process. Adsorption capacities as high as about 900 mg/g have been reached for Cr^{3+} removal from water using an agro-industrial residue as precursor for AC. Different raw materials (from petroleum pitch to agricultural residues), processing parameters and removal conditions have been studied, focusing on reducing the cost of treatments using AC, increasing its adsorption capacity, developing environmentally friendly activation processes, improving the operational life and recyclability.

1.3.4.3. Polymeric materials

Polymeric materials offer high stability and processability, and provide specific bindings to target pollutants when they are used as matrices. These materials are malleable, easy to functionalize, and their structure can be tailored to significantly enhance the adsorption properties. However, given the pollution associated to the use of some polymers, governments and industries demand environmentally friendly materials. Features such as cost-effectiveness, non-toxicity, biodegradability, biocompatibility, reusability, and ease of synthesis, preparation or extraction are among the characteristics that a material to be used for pollutant removal should have. These key characteristics are commonly present in many natural polymers, such as alginate, silk, lignin, chitosan, and cellulose. Alginate composites, for instance, exhibit good removal capacity of dyes, heavy metals, and other water pollutants Lignin-based materials can achieve removal efficiencies from water higher than 90%. Likewise, chitosan and cellulose-based materials are extensively utilized for water remediation, and as part of different techniques for the removal of oils, grease, and heavy metals. In particular, cellulose is the most abundant natural polymer available, shows a huge variety of unique biological and physio-chemical properties, and fulfills several expectations of a suitable agent for water remediation Thereby, biopolymers emerge among the most suitable materials for remediation applications.

1.3.4.4. Agricultural residues

Agricultural residues are mainly composed of hemicellulose, cellulose, lignin, and starch, which are biopolymers showing strong exceptional adsorption capacities and possess a great variety of functional groups that allow metal complexation. In

addition, one of the main advantages of these biosorbents is that they can be readily modified to enhance their adsorption capacities and their adaptability at in. These residues, or their byproducts, are also less expensive, highly efficient and minimize chemical or biological sludge when compared to conventional remediation. The effectiveness of these residues depends on parameters such as pH, temperature, adsorbent dose and concentration of heavy metals.

1.3.4.5. Industrial wastes

Industrial wastes have been used to remove heavy metals from wastewater because they are low-cost, widely available, and high-performing. These materials include sludge, blast furnace slag, flue dust, fly ash, lignin and red mud For instance, it has been shown that sludge can effectively remove $Pb^{2+,}$ $Cd^{2+,}$ Cr^{3+} red mud can remove Cu^{2+} from wastewater, and organic acids can be used to extract Cu^{2+} and Zn^{2+} from sewage sludge so that the sludge can be recycled. To improve the removal efficiency, researchers typically tune operation parameters, such as contacting time, dose, temperature, pH, ionic strength and initial metal ion concentration.

1.3.4.6. Magnetic adsorbents

Magnetic adsorbents can be readily separated from an aqueous solution by applying an external magnetic field. This is an advantage that could lead to more efficient water treatment processes while potentially reducing their cost, and it is also one of the reasons for studying the removal of pollutants from water using different magnetic particles, nanoparticles and composites. Some examples include zero-valent iron, iron oxides such as hematite (a-Fe_2O_3), magnetite (Fe_3O_4) and maghemite (y-Fe_2O_3), and spine) ferrites. When these iron oxides are used as nanoparticles, they are very effective due to their large specific surface area, numerous active sites, extraordinary surface charge and redox activity. Moreover, most of these magnetic nanoparticles are easy to synthesize, considered non-toxic, and inexpensive Additionally, they can be synthesized through a variety of sustainable methods, even using natural precursors, as in the case of ilmenite ores (FeTiO3).

1.3.4.7. Composite adsorbents

Composites are promising adsorbents, as several studies have demonstrated. Their advantage lies on the possibility of combining two or more materials to obtain an adsorbent with properties that are better than those of its constituents. For instance, lignocellulosic sawdust residues (LR) were impregnated with magnetite nanoparticles (MNP) to obtain composites with LR:MNP ratios of 1: 1 and 3:1. The adsorbents prepared required shorter contact times to achieve the same high

removal efficiencies obtained with the nanoparticles or the residues by themselves. Additionally, since the adsorptive removal performance was similar for both composites, it was found that relatively large amounts of the low-cost LR could be combined with small quantities of costly MNP to obtain highly efficient adsorbents. On the other hand, chitosan and alginates have been used to functionalize AC to obtain composites with high mechanical strength, improved durability, better hydraulic properties, and high affinity for several pollutants AC has also been impregnated with magnetic nanoparticles to adsorb several metallic ions, including Pb^{2+}, $Cd^{2+,}$ $Cu^{2+,}$ Zn^{2+}, $Ni^{2+,}$ Cr^{6+}. Magnetic biosorbents can efficiently eliminate heavy metals and other inorganic and organic contaminants 2020). For instance, magnetite/maghemite nanoparticles embedded in a chitosan matrix exhibited relatively high adsorption capacities, such as 221 mg/g for $Pb^{2+.}$

1.3.4.8. Microbial fuel cells

Microbial fuel cells (MFCs) represent a promising technology because they use organic matter present in wastewater to produce electricity via biocatalysts such as microbes. In MFCs, the microbes produce protons and electrons on the anode cell (anaerobic), which transfers the protons through a proton exchange membrane and the electrons through the external circuit to the cathode cell (aerobic). At the cathode, oxygen closes the circuit and reduces to water due to its high redox potential. Heavy metal removal using MFCs allows heavy metals with higher redox potential than the anode electrode to be removed and recovered in the cathode chambers MFCs have even been used for in situ remediation in rivers, in which the results showed removals of 97.3% $Hg^{2+,}$ 87.7% Cu^{2+} and 98.5% Ag^{1+} after 60 days of MFC operation. Furthermore, MFCs effectively enhanced the biodegradation of organic matter, generated electricity and provided an alternative approach for efficiently remediating contamination of multiple heavy metals with simultaneous bioenergy recovery.

1.3.4.9. Nanotechnology

Nanotechnology-based treatments use nanomaterials, which have gained special attention in the last decades because of their high surface-to-volume ratios and unique electronic, optical, and magnetic properties. Nanofiltration is among the most used nanotechnology processes for heavy metal removal. Systems based on alumina nanofibers are highly efficient for removing dissolved heavy metals via chemisorption. Moreover, low dimensional structures such as nanocarbon, single or multi metal oxides, non-metal oxides, magnetic nanoparticles and nano clays are the most used for the purification, disinfection, and removal of heavy metals from water. All these nanostructures exhibit highly reactive and large surface areas, and many of them are abundant in nature or have low-cost synthesis processes.

Similarly, nano-assemblies, nanoplates, microspheres with nano-sheets and hierarchical ZnO nano-rods have been used for wastewater treatment. However, the scarce information about the toxicity, environmental and health effects of nanomaterials is considerable and impedes their full exploitation.

1.3.4.10. Nanocarbon (carbon nanotubes, graphene and other carbon derivatives)

Nanocarbon, either as carbon nanotubes (CNTs), graphene or its derivatives, is used as a highly efficient adsorbent. The carbonaceous nature of CNTs and their highly reactive surface area may allow direct interaction with water pollutants through hydrophobic, n-n, covalent, hydrogen bonding and electrostatic interactions. Moreover, their rod-like and hollow shape make them exceptional for water remediation, offering several possibilities for adsorption to take place. Although challenging, the properties of CNTs can be transferred to the macroscopic world by preparing composite materials formed as fibers, reinforced polymers, films, gels, and aerogels. The CNT surface can be easily modified through acid treatment, metal impregnation and functional molecules/group grafting. The latest, allows the control of the nanotube surface area, surface charge, dispersion and hydrophobicity and their concomitant adsorption potentials. For heavy metal removal, hydrochloric, nitric, or sulfuric acid functionalization introduces oxy functional groups which are highly effective for removing wastewater pollutants such as cadmium, copper, lead and mercury.

Graphene is another promising material for water treatment. Its morphological flat and two-dimensional (2D) honeycomb atom arrangement, accompanied by its hybridized sp2-structure and the associated electronic band structure, can be easily modified for custom made functionalities Chemical oxidation of graphene is readily achieved through acid functionalization producing hydrophilic and carboxylic acids which increase dramatically its adsorption of heavy metals Graphene oxide (GO) based materials, including those chemically modified and composites, have been used in heavy metal removal applications. Other graphene derivatives as its reduced form (RGO) are being used successfully for water treatment. For instance, 3D graphene-based macrostructures offer a large surface area and porous network, accompanied by high electronic mobility, excellent chemical active sites, and ultra-lightness. These structures can also serve as scaffolds to immobilize nanomaterials which significantly broadens their potential applications in any water treatment, scaffold doped with graphene oxide flakes (GOFs) and showed its potential for removal of Pb2+ and As3+ ions from groundwater samples. These GO-based mesoporous materials allowed being recycled four times without any effective loss in activity

1.3.4.11. 2D materials

2D materials, also known as single-layer materials, include graphene and borophene, germanene, silicene, 20 metal carbides (MXenes), MoS2 nanosheets, among others. MXenes have unique layered structures, oxidized functional groups, and active binding sites, which make them unique adsorbents for removing heavy metals from water (Feng et al., 2020). The most studied MXene is $Ti_3C_2T_x$, which has been used in a variety of ways, from nanosheets to composites. The 2D MXene-based materials have shown high sorption capacity, fast kinetics, and very high removal efficiencies, being competitive with commercial adsorbents such as AC under a wide range of conditions .MoS_2 based materials are popular and high performance adsorbents; their S atoms have good affinity with heavy metals, while Mo provides enhanced catalytic performance in the degradation of organic pollutants MoS_2 nanosheets have been suspended in aqueous solutions, stacked as thin-film membranes, and incorporated in composites. In all these cases, these materials have shown fast kinetics, high adsorption capacities and efficiencies.

1.3.4.12. Nanoparticles

Silicon, iron, titanium, zinc, magnesium, and manganese oxides are commonly used for heavy metal remediation in the form of nanoparticles. Silica nanoparticles have high porosity and silanol groups on the surface, which can be easily modified via silane chemistry. Silica nanoparticles, by themselves, combined with materials such as GO, or functionalized, can efficiently remove metal ions such as $Ni^{2+,}$ Pb^{2+} and Hg^{2+} ion oxide nanoparticles (IONPs) are magnetic materials that can be conveniently used to remove and separate heavy metals. The most used are based on ferric oxide nanoparticles mainly due to its large surface charge, high redox potential, and its reusability. The hydroxyl groups on the surface of IONPs render the capability for surface modification. As in the case of silica, IONPs can remove a variety of heavy metals and its adsorption performance can be improved via functionalization (Al-Saad et al., 2012; Warner et al., 2010). TiO_2 nanoparticles have catalytic properties superior to their bulk counterparts. These nanoparticles can adsorb metals and metalloids such as $Zn^{2+,}$ Cd^{2+}, As^{5+}, Cr^{6+}, La^{3+} and $Nd^{3+.}$

Both biological and chemical non-conventional methods for the removal of heavy metals have advantages and disadvantages. Although there is a large effort in developing nanotechnologies and few products available for the removal of heavy metals, their use remain a challenge mostly due to the cost. Biological methods seem to have a higher acceptance due to the environmentally friendly nature and low cost.

1.3.4.13. Commercial products for heavy metal removal

A continuously increasing group of commercial products have been tested, developed, and used for heavy metal removal. An important portion of these products is composed by adsorbents, which are part of relatively mature technologies. Powdered, granular, layered, and fiber materials have been formulated and extensively studied during the last few decades. Activated carbon is perhaps the best known and it is typically obtained using precursors such as coal or agro-industrial residues (e.g. wood, coconut shells, bamboo). Several products based on nanoparticles and nanocomposites have also entered the world market.

1.3.4.14. Fenton-like reactions

The Fenton reaction is an advanced, naturally occurring oxidation process, that has been developed in recent decades for the degradation of various contaminants. Hydroxyl radicals that are generated from a mixed solution of H202 and ferrous ions have oxidizing properties, which allow efficient oxidation of many organic compounds in inorganic forms.

In this reaction, soluble iron cations interact with H_20_2 to generate OH, which allows the degradation of complexes of metallic organic matter.

The Fenton reaction alone has demonstrated not to be sufficient for wastewater treatment, as it does not meet established standards to be an industrially scalable method. However, continuous research and development have allowed the optimization of this technique. In particular, the use of combined methods offers efficiency improvements because it allows a greater selectivity of reaction and formation of OH, decreases the reaction time and activation energy, in addition to allowing the simple reaction. For instance, bioleaching in combination with Fenton reactions was investigated for sludge treatment in terms of heavy metal removal. The combined process led to very high improvements in sludge dewatering. The disadvantages of this treatment include that it works within a narrow pH range, generating large amounts of iron residue, having high operational costs and low water volume treatment capacity. Therefore, this method requires further research to produce an improvement and optimization that reduce the economic burdens.

1.3.4.15. Plant-mediated remediation of heavy metals

Phytoremediation is one of the most used techniques to eliminate heavy metal pollution in ecosystems or environments. It uses raw or genetically modified plant

species to minimize the toxic effects of pollutants Plants are often combined with other living organisms (bacteria, fungi, algae, biofilms, plants), other external processes (thermal, physical, chemical, electrical) or inputs (soil amendments, macro-micro nutrients, fertilizers, plant-litter, nanocomposites, biosurfactants, emulsifiers, sorbents, gels, hydrogels, ceramics, clays, water, aeration, etc.), to remediate contaminated ecosystems A series of emerging complementary processes and methods can be used to enhance the efficiency of this technique, as well as to overcome current drawbacks. However, phytoremediation efficiency depends not only on technical factors, but also on logistics, infrastructure, time and costs. Phytoremediation is environmentally friendly, can operate at large scales, has low installation and maintenance costs, and contributes to the conservation of soil and ecosystem structure, prevention of erosion and leaching of metal. The possibility of Phyto mining, which is the recovery of bioaccumulated metals, is also one of its advantages. Additionally, phytoremediation can contribute to the generation of local employment.

A heavy metal plant-mediated remediation framework could be summarized in 4 phases. These 4 stages are: (1) Preliminary considerations, (2) processes, (3) state-of-the-art phytoremediation and (4) final disposal of heavy metals. The main aspects to be addressed during the first phase include: (a) identifying the ecosystem polluted; (b) defining the heavy metals physio-chemical characteristics, including volume, surface, interactions with other chemical compounds and their environment; (c) choosing the plant and the living organisms' association .Some elements to consider during the selection of a phytoremediator plant are: its root system, biomass above the ground, growth rate, contaminant toxicity for the plant, adaptability to the environment, and the time required to reduce the contaminant concentration to a desired level. The plant should also be tolerant to diseases and pests.

Once the magnitude of the pollution is assessed, during the second phase, it is necessary to choose an affordable process to remediate it. In phase 3, we analyze the use of cutting-edge technologies, many of which are based on nanotechnology. For example, the plants could absorb the metals from the growth media, reduce them to nanoparticles through their metabolic pathways, and store them in stem, leaf and roots. Plants labeled as phyto-tolerant or phyto-accumulators, reduce the toxicity by preventing the translocation or destroying the contaminants.

During the last phase, the final disposal of heavy metals, their subproducts, and residues is analyzed. This disposal could be efficient and economically viable if the post-harvesting technologies employed are properly chosen and applied. From the options available, valorization of residues or materials with high content of heavy

metal has received special attention worldwide, due to the positive technical, environmental and economic results (circular economy-sustainable development). A recent study addressing this topic demonstrated that the combination of biosorbents with catalytic technologies provided new ideas for future research about biosorption. In previous sections, we have discussed the principal mechanisms and methods that can be used to remove heavy metal and metalloid ions from water. As a result, it is possible to say that there is no technology that can guarantee easy and low-cost implementation, cost effective and environmentally friendly operation, while maintaining high efficiencies in the wide variety of settings that demand the elimination of water pollutants. For this reason, we would like to summarize the main features of the methods studied, highlighting their weaknesses and strengths. In general, the conventional methods entail a combination of physical, chemical and/or biological processes. However, only a few of them are currently employed by the industrial sector due to technological and economic concerns for example, membrane technologies offer high removal efficiency and reduced energy consumption, but exhibit some disadvantages such as membrane fouling and lower permeate flux, which in turn would rise the implementation costs. According to the literature, treatments based on chemical precipitation have simple operation processes and relatively easy automatization. However, one the main drawbacks of this method consists on the production of a large amount of toxic-sludge, that requires further treatments. On the other hand, non-conventional treatment and emerging removal methods, from adsorption to microbial fuel cells, including nanotechnology approaches, and Fenton like reactions, have the higher implementation costs as one of their main inconveniences. The use of nanotechnology to fabricate tailored macroscopic materials based on nanoparticles, hybrid organic/inorganic composites have gained special attention in the last decades because their physio-chemical features, promoting better performance during sorption and sorption reduction processes. This is a key point in most of the remediation techniques. Combining the best adsorbent with the correct molecule will be a promising route to high performance, cost-effective and reliable treatment methodologies. Many efforts have been dedicated to conceive sustainable remediation methods using industrial and agro-industrial wastes, aiming to take advantage of the beneficial environmental, economic and social features of these materials. However, these initiatives have faced several drawbacks such as the expensive pretreatments required for conditioning the residues, or constraints like the enormous distances between the industrial and agro-industrial waste source and some of the locations for the water treatment. Fenton-like reactions offer selective efficiency improvements; however, they should be combined with other technologies to fit the requirements of industrially scalable methods. Finally, plant remediation technologies benefit from

the use of living organisms and inputs such as soil to remediate contaminated ecosystems and minimize the toxic effects of pollutants. However, they must be applied in combination with other technologies to be more efficient and competitive.

2. Literature review

2.1.literature review on Sol-Gel method

2.1.1. Sol–gel-based aerogel synthesis

The sol–gel method is the most widely used and perhaps simplest method for the synthesis of inorganic, carbon and composite cryogels, xerogels and aerogels. This process involves the following steps.

2.1.2. Sol preparation

Depending on the choice of base material, stable metal salts oxides/alkoxides or organic—are dissolved in a suitable solvent containing water, ethanol, methanol, or a mixture of these. Upon vigorous mixing, dissolution of the metal oxide/metal salts will result in a colloidal suspension with a particle diameter ranging from 1 μm to 1 nm[1] .

2.1.3. Gel formation

The colloidal suspension is converted into a gel by crosslinking the metal oxide solution through self or induced polycondensation reactions. This produces a three-dimensional (3D) interconnecting network of irregular shapes. The gel will mostly contain the 3D metal oxide network and solvent-filled pores. To initiate the gelation process, the pH or temperature of the sol must be adjusted to optimal values.

2.1.4. Aging

The formed gel is kept for a few hours to several days at varying temperatures in a controlled air oven, to increase polymer crosslinking ([2]. High crosslinking will result in a good aerogel material with excellent pore size and a large surface area. During aging, gel cracks should be avoided, as these lead to poor aerogel formation.

2.2.literature review for drying methods

2.2.1. Drying

Drying is the final stage in aerogel synthesis. It provides the desired shape of the material and constitutes a significant step in controlling the physicochemical properties of the aerogel. In the hydrogel/alcogel drying process, air (or a suitable gas) replaces the water/solvent without collapsing the 3D hydrogel/alcogel structure ([3]). Three common drying processes are ambient pressure drying, freeze drying and supercritical drying.

2.2.1.1. Ambient pressure drying

In ambient pressure drying, the solvent in the gel pores is removed without the need for additional solvent, at least in theory. However, pore shrinkage can occur during

removal of the solvent occupying the pore space in the gel; during evaporation, surface tension induced in the liquid surface of the pores at the solid–liquid–vapor interface can result in capillary tension on the pore walls. If the shrinkage is severe, the walls of the pore will come into contact with each other, leading to reactions between the surface groups and gel collapse. To avoid shrinkage and collapse, it is important to stop or reduce the capillary stress developing in the pore walls ([4]). This can be achieved by chemically treating the pore-wall surfaces with nonpolar groups to prevent further condensation due to surface charges ([5]). Thus, ambient pressure drying relies on surface passivation through modification, usually silylation, of the internal gel surface, before the actual drying procedure can be performed, thereby preventing the condensation of reactive groups on the pore walls during drying, and resulting in better porosity. Moreover, an exchange of the pore-filling solvent with a hydrocarbon or a solvent with less surface tension is required to avoid the capillary stress on the pore walls. Thus, the additional organic solvent used in this step does constitute a form of solvent exchange, even with the use of a drying method that does not, theoretically, include such a step. Conventional ambient pressure drying enables large-scale production of aerogels at low cost ([6]), compared to the high cost and time-consuming process of large-scale production of aerogels using supercritical drying or freeze drying. On the other hand, these latter techniques have certain advantages.

2.2.1.2. Freeze-drying (lyophilizer) process

High-temperature or ambient-temperature drying may not be suitable for certain solvents, for various reasons. The next step after the gel formation is drying. The gel is dried by the freeze-drying method which is a low temperature drying method specifically used to prepare aerogels with a small 3D porous structure. In freeze-drying, freezing the liquid inside the gel is followed by the removal of the liquid inside the gel using a sublimation process ([7]). Freeze drying is a three-step process: first, the temperature of the sample is lowered below the triple point of the pore-filling solvent usually water the second step is vacuum applying to lower the pressure and develop a gradient and the final step is the sublimation of the frozen gel under controlled isobaric conditions. The freeze-drying process around the liquid–gas boundary is accompanied by low temperature and low pressure. However, some structures can be disrupted, even by the solid–gas boundary ([8]). The freeze-drying mostly results in aerogel materials with a microporosity, and even though most of the freeze-drying produces aerogels, still some of them do not attain the aerogel quality and result in open porous foams known as cryogels ([9]). Recently, after careful optimization of the freeze-drying process, the porosity of the aerogels reached more than 99% ([10]), and in some cases, it reached a maximum of 99.9%, which are highly competitive to the super critically dried aerogels. In

some cases, the quick freezing of the cryogels yields a high proportion of microporosity, shrinkage, and a low specific surface area compared to the aerogel obtained by supercritical drying. Most commonly supercritical drying of hydrogels/alcogels efficiently removes the solvent in the gel without disturbing the 3D network structure. On the contrary, the ambient atmospheric drying of gels results in xerogels in which the pores usually collapse during the drying process due to the high capillary pressure ([11]). On the other hand, freeze drying of hydrogels leads to the formation of cryogels, which results in more structural deformation and possibly larger pore size due to the amplification in the volume of water upon crystallization ([12]). But, massive aerogels with modest textural properties were reported using the freeze-drying techniques: the microporosity upon the freeze-drying would be avoided by increasing the cooling rate of the hydrogel precursors with liquid propane or spraying freeze drying methodology. Another possibility to produce an aerogel by freeze-drying method is using the alcogels instead of hydrogels which result in an enhancement in the microporosity of aerogels compared with the hydrogel counterparts ([13]). This low-temperature process is also known as cryodesiccation, lyophilization and ice-templating. Most of freeze-drying follows the sol-gel method in which the gel is either prepared from water or alcogel solvent. The main setback of the sol-gel method is gelation. To get a perfect gel, various parameters should be tuned such as buffers or pH adjustment, capping agents or cross-linking molecules. This will make additional charges and time consuming in the aerogel synthesis. These drawbacks were eliminated by direct freeze-drying methods. In 2017, Burpo et al., reported a rapid, direct solution-based reduction synthesis method for the gold, palladium, and platinum aerogels ([14]). Several directly freeze-dried aerogels are available for the application of water remediation purposes ([15]). Nanofabricated cellulose aerogel functionalized with silver nanocomposite was synthesized by direct freeze-drying method and used for catalytic degradation of rhodamine B ([16]). According to IUPAC, the aerogel is defined as follows, “A gel comprising a microporous solid in which the dispersed phase is a gas”; where the precursor for the aerogel must be a Gel. Whereas in 2021, Wang et al., reported a cellulose aerogel from the nano-cellulose suspension using direct freeze-drying followed by thermal induced cross-linking. The aerogel synthesis protocol is as follows: (1) nano-cellulose was mixed uniformly in a 1 mL polyamide-epichlorohydrin resin solution (~0.125 wt%), and the solution underwent directional freezing in liquid nitrogen for 5 min; (2) the frozen sample was freeze-dried and heated at 80 ◦C for 12 h in a vacuum to obtain cross-linked nano-cellulose aerogel, and (3) the synthesized cellulose aerogel was used as an effective adsorbent for uranium (VI) from an aqueous solution ([17]. Even though a massive number of reports are available for the aerogel synthesis

using freeze drying method the main setback is the higher cost compared to ambient pressure drying.

2.2.1.3. Supercritical drying

In supercritical drying, the solvent inside the pores is removed in a controlled manner, resulting in aerogels with a good structure and high porosity and surface area. A supercritical fluid (SCF) is used as the cosolvent in the drying process, overcoming the problems encountered with conventional drying methods and preserving the 3D, high open porosity and superior textural properties of the wet gel in dry form. In this process, a solvent-rich gel is positioned inside a high-pressure batch reactor and exposed to natural gas such as methane or carbon dioxide (CO2). The reactor temperature and pressure are maintained above their critical points It is crucial to have the solubility data for the solvents in the SCF. A proper mass balance of the solvent in the gel and a suitable size of the reactor holding the SCF are essential for better drying. The SCF has a liquid-like density that can be tuned (by changing the operating temperature and pressure) to increase or decrease the solubility of the solvent in the pores, imparting versatility to the overall process ([18]). Operational temperature and pressure are set so that the solvent in the pores will dissolve in the SCF; the gas-like viscosity of the SCF then allows the solvent to efficiently diffuse out through the pores, resulting in a solvent-free xerogel. The use of SCF also avoids the coexistence of vapor and liquid, thus eliminating the surface tension and capillarity phenomena associated with such systems. The supercritical-drying process thus prevents pore collapse of the solvent-filled gel structure during solvent elimination ([19]). Super critically dried aerogels are superior to freeze drying and ambient pressure drying due to the quality, purity, surface area and porosity, however, production cost in supercritical drying is higher.

2.3. Comparison between various drying methods

Table 2:Drying method comparison

Sl no.	Properties	Super critical drying	Freeze drying	Ambient pressure drying	References
1	Nature	c**rystalline or amorphous**	**Crystalline or amorphous**	**Amorphous**	[20], [8] and [21] and [22]

2	Cost	expensive	Less expensive	Inexpensive	
3	Purity	high	high	low	
4	Environmental Effect	Benign	Benign	Benign	
5	Availability	Less available	Less available	Easily available	
6	Degradation	Absence	Absence	Presence	
7	Recyclability	Easy	Easy	Difficult	

2.4. Literature Review of CNC based aerogel for heavy metal ion removal

Table 3: Literature review

Adsorbent	**Crosslinking strategy and/ or Functionalization**	**Adsorption Conditions**				**Contaminant Removed**	**Removal (mg/g)**	**Computation Model (R^2 Data)**	**Recyclability**	**Reference**
		Concentration	**Temp (ºC)**	**Time (hr)**	**pH**					
TEMPO-CNC Aerogel	Guanidine-functionalized sericin/nanocellulose aerogel	0.1 g of the aerogels were immersed in 200 mL of 10 mg/L	25	12	2–6.5	Cu(II)	571.5	Langmuir (0.9942)	82.6% after 10 consecutive cycles	[23]
						Co(II)				
						Ni(II)				
Nanocellulose	Compounded with	20 mg of aerogel sample	25	24	2-10	Cr(VI)	350.64 (93.86%)		81.86% (After 6	[24]

Aero gel	MOF-801	s in 20 mL of 50 mg/L							cycle s)	
Chemically crosslinked Cellulose Aerogel	polydiacetylene (PDA) developed on Cellulose Aerogel (hydrazone bonded CHO-CNC and NHNH2-CMC) with 2D heterojunctions (ZnO/MoS2)	NA	25	3	NA	VOC(Toulene)	97% ***degradation***	NA	NA	[25]
Fixed Bed Experiments with Hollow Beads										
Packed bed with CS@CNC−HTA Chitosan beads	1:1 CS@CNC− HTA beads (CNCs and hydrophobic tannic acid (HTA) composite contained in hydrophobic chitosan (CS) beads)	50 mg/L		14.8	6	pharmaceutical sildenafil citrate	86 (73%)	NA	NA	[26]
		100 mg/L		5		basic blue 26 dye	375 (84%)			
		100 mg/L		7.8		Surfactant cetylpyridinium chloride	390 (90%)			

Packed bed with CS-Fe@PEI beads	Cellulose Nanofbers(CNF), sodium alginate(SA), and polyethyleneimine (PEI) cross linked with ferric chloridea nd glutaraldehyde	0.020 g of beads were added to 20 mL of initial concentration 500 mg/L	25	24	2	Cr(VI)	526.32	Langmuir (0.999)	91.68% after five cycles	[27]
Hydrogel										
Lignosulfonate-Based Hybrid Hydrogels	Polyamide Amine crosslinked with lignosulfonate mine with poly(ethylene glycol) diglycidylether (PEGDGE)[1:4]	20 mg of adsorbent in 25 mL of initial concentration 6000 mg/L	25	24		Congo Red	5120	pseudosecond-order (0.98078) and Langmuir (0.9386)	NA	[28]
		20 mg of adsorbent in 25 mL of initial concentration 100 mg/L				Cu(II)	249	pseudosecond-order (0.98612) and Langmuir (0.9982)		
biodegradable	corn starch-based	100 mg hydrogel (5	NA	3	3	Cu(II)	20.3	Fick's diffusion	Sample biode	[29]

composite hydrogel	hydrogel with nanocellulose content	wt% nanocellulose) in initial concentration of 25 mg/L		1		Cr(VI)	3.5	model (0.942)	graded	
Static and dynamic dye removal										
Cellulose based aerogel adsorbent	Cellulose acetoacetate and β-cyclodextrin acetoacetate polymer chains crosslinked using polyethyleneimine (PEI)	50 mL of initial concentration 500 mg/L	25	24	7	Methyl Orange	1013.11 (98.9 %)	Langmuir (0.999)	Loss of 16% adsorption capacity in second cycle	[30]
Bacterial cellulose (BC)/poly(amidoxime) (PAO) aerogel		.1g in 20ml solution	NA	30min	6	Pb^{2+}	571.5	Langmuir (0.999)	NA	[31]
						Cu^{2+}	509.2			
						Zn^{2+}	494			
						Mn^{2+}	457.2			
						Cd^{2+}	382.3			

TEMPO-oxidized CNFs aerogel						U(VI) (Static adsorption)	440.60			[17]
						U(VI) (Dynamic adsorption)	194			
Bentonite modified chitosanmicrocrystalline cellulose aerogel						Pb(‖)	256.24			.[32]
(CNC-PVAm/rGO)						DCF	450.49			[33]
GO-CEL-Cu						MG	207.1			[34]
PEI-AgNCs /CNC						Cr(VI)	0.20 ± 0.03 g			[35]
CNF/GO						MB	91%			[36]
PEI@CNF aerogels						$Cu^{2+,}$	86% 135.1 mg/g			[37]

PMV EMA /PEG/ CNC						MB	116.20 mg/g			[38]
Alginate Gel Beads with Cellulose Nanomaterials						Cu^{2+}	53.4			[39]
						Pb^{2+}	76.8			
						Mg^{2+}	68.4			
						Fe^{2+}	234.8			

2.5. Aims and Objectives

Cellulose-based aerogels, a new class of porous materials, have emerged as a promising technology for wastewater treatment. Derived from renewable and abundant sources such as plant biomass, cellulose-based aerogels exhibit unique properties such as high surface area, low density, tuneable porosity, and excellent mechanical properties. These characteristics make them highly effective in adsorbing pollutants from wastewater.

2.5.1. Aim

The aim of this work is to fabricate nanocellulose based aerogel for the remediation of heavy metals present in waste water.

2.5.2. Objective

The specific objectives of this work is

- **Design and Fabrication of High-Performance Aerogels:** The first objective is to develop cellulose-based aerogels with optimized physical and chemical properties for efficient pollutant removal. This involves tailoring the pore structure, surface area, and mechanical strength to maximize adsorption capacity for contaminants such as heavy metals (e.g., copper and chromium).
- **Achieving High Adsorption Capacity**: A key objective is to achieve high adsorption capacities for various pollutants, comparable to or exceeding existing treatment materials. This requires research into the modification of

cellulose aerogels with functional groups (e.g., carboxyl, hydroxyl, or amine groups) that can enhance their affinity for specific pollutants.

- **Developing Functionalized Aerogels for Targeted Applications**: Functionalization of cellulose-based aerogels through chemical treatments or the incorporation of nanoparticles (e.g., metal oxides) can enhance their capacity for specific pollutants. The objective is to develop aerogels that are selective for certain contaminants, such as heavy metals like Cu, Cr, improving the overall efficiency of wastewater treatment.
- **Improving Durability**: Another technical objective is to improve the durability of cellulose-based aerogels. Since these materials are often designed for use in multiple treatment cycles, enhancing their mechanical stability and resistance to chemical degradation is crucial for reducing costs and improving performance in real-world applications.
- **Isotherm and Kinetics of the System**: Isotherm fitting and kinetics of the system evaluation is the final objective of this work. Various isotherm like Langmuir Freundlich etc will be fitted to the experimental data to categorize the adsorption data obtained during experiments and finally the first order, second order kinetics data will be fitted.

3. Experimental Methods

3.1. Experimental Design

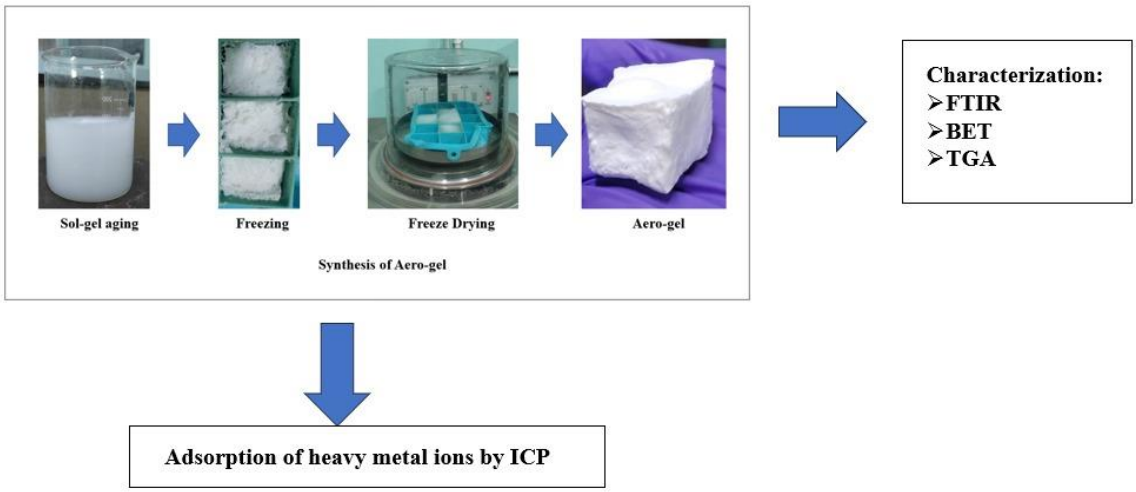


Figure 1: Experimental design

3.2. Materials & methods

All the chemicals used in this work were of analytical grade and used without further purification. Powdered CNC(cellulose nano crystal) was purchased from ICAR-CIRCOT, Pune, India. Sodium meta periodate ($NaIO_4$), polyethylene glycol (PEG 400), Polyethylene amine (PEI), Copper sulfate and potassium dichromate were all purchased from Sigma Aldrich.

3.2.1. Fabrication of nano cellulose aerogel

The functionally modified CNC aerogels were prepared through a freeze-drying method. First, 2 wt% CNC was dispersed in 100ml deionized water (DI), making a slurry, and then the desired amount of $NaIO_4$(1gm) and 1gm of PEG (as crosslinking agent) was added followed by thorough stirring for 4 h to obtain a homogeneous mixture. Then 1ml glutaraldehyde (as a binding agent) was added to the mixture and stirred for an hour. The solution was rested for another 2 hours for gelation. After aging excess water was decanted and the gel was placed into a Silicone square-shaped mould (0.5 cm diameter and 2.5 cm height), subsequently frozen in a deep freezer for 12 h, and freeze-dried (Labogene Coolsafe -110°C) for 24h. Because of the freeze-drying process, the ice in the CNC-NaIO4 /Glutaraldehyde (S1) was removed, leaving macropores. This process resulted in a 3-dimensional sponge-like surface-modified CNC-aerogel.

Similarly, for preparation of S2, 2 wt% CNC was dispersed in 100ml DI, making a slurry. Next, the desired amount of $NaIO_4$(1gm) and 1gm of PEG (as crosslinking agent) was added and stirred thoroughly for 4h to obtain a homogeneous mixture without any binding agent, it was then freezed and then freeze-dried for 24 h in the same silicone mould setup.

For S3, the same Sol-Gel process was used as S2 with the addition of 1 gm of PVA as a binding agent, and the same freeze-drying technique was used to obtain the aerogel.

In the case of (S4), 1gm of PEI was added with 2 wt% of CNC in 100ml DI. It was stirred for 3 hours with a pulsating heat and subsequently sonicated for 30 mins. The solution was rested for 2h and excess water was decanted after aging. Subsequently, it was transferred to a silicone mould and then froze. After freezing the ice crystals were removed by freeze drying leaving behind a PEI/CNC Porous aerogel.

Again, in S5, for aldehyde modification 1gm of $NaIO_4$ was added with 2wt% CNC and as crosslinking agent PEI was used. Similar Sol-Gel and freeze-drying technique with same conditions (Previously mentioned) were used here for the formation of aerogel.

For S6, the exact process of S5 was used in addition with 1gm of PVA as binding agent and pulsating heat was applied during the solution stirring. The details of all the samples are summarized in Table 4.

Table 4: Sample components

Sample ID	Precursor	$NAIO_4$ (amount)	Crosslinking agent	Binding agent	drying	Time
S1	CNC(2wt%)	1gm	PEG (1gm)	Glutaraldehyde (1gm)	Freeze drying	24hr
S2	CNC(2wt%)	1gm	PEG (1gm)	NA	Freeze drying	24hr
S3	CNC(2wt%)	1gm	PEG (1gm)	PVA(1gm)	Freeze drying	24hr
S4	CNC(2wt%)	NA	PEI(1gm)	NA	Freeze drying	24hr
S5	CNC(2wt%)	1gm	PEI (1gm)	NA	Freeze drying	24hr
S6	CNC(2wt%)	1gm	PEI(1gm)	PVA(1gm)	Freeze drying	24hr

3.2.2. Characterization of prepared Aerogels

All the samples were subjected to several optical and morphological studies. FTIR(Jasco) was mainly used as a qualitative technique for the study of the surface chemical functional groups present on the aerogel surface. To check the porosity, specific surface area, void volume of the aerogels BET was done. Thermal stability of the samples was checked by TGA. Also To check the ionic concentration of metal ions in the solution, ICP -OES was used.

3.3. Batch adsorption Experiment of Cu

1000ppm $CuSO_4$ solution was prepared by mixing 1 gm of $CuSO_4$ in 1 liter of distilled water. This solution was further diluted to 10 ppm solution and adsorbent dosage of 1g/L was used for various CNC-aerogel. The diluted solution was divided into six conical flux of 100 ml with different aerogel samples and were transferred into a BOD shaker at a temp of 25°C for 24 hours. After that 10 ml samples were taken out from each conical flask and to detect the ionic concertation, ICP-OES was carried out. During sample preparation the solutions were passed through 0.22micron syringe filter to mitigate any possibilities of contamination.

Out of the six samples of prepared CNC-aerogel, best four samples were selected and then the solution pH was varied from 2-10 and the same process was followed as before for adsorption studies. The best pH data for the best adsorbent sample was further selected for the experiment.

The dosage amount of the best proven sample at a certain pH was varied with different dosage of the adsorbent (0.25g/l, 0.5g/l, 1g/l, 2g/l) in 10PPM $CuSO_4$ and after 24 hours ICP was done to find the best dosage amount.

3.3.1. Batch Adsorption Experiment of Cr(VI)

1000ppm $K_2Cr_2O_7$ solution was prepared by mixing 1 gm of $K_2Cr_2O_7$ in 1 liter of distilled water. This solution was further diluted to 10 ppm solution and adsorbent dosage of 1g/L was used for various CNC-aerogel. The diluted solution was divided into six conical flux of 100 ml with different aerogel samples and were transferred into a BOD shaker at a temp of 25°C for 24 hours under continuous stirring. 10 ml samples were taken out from each conical flask and for detection of ionic concertation using ICP-OES was done. During sample preparation the solutions were passed through .22micron syringe filter to mitigate any possibilities of contamination.

Out of the six samples, best four samples were selected and then the solution pH was varied from 2-10. The adsorption was carried out using 1g/l dosage and for 24h. The Cr concentration in the solution was detected using ICP-OES. The best pH data for the best adsorbent sample was selected for the further experiment.

The dosage amount of the best proven sample at a certain pH was varied (0.25g/l, 0.5g/l, 1g/l, 2g/l) for 10ppm $K_2Cr_2O_7$ and after 24 hours ICP-OES was done to find the best dosage amount with highest removal efficiency.

3.3.2. Adsorption Studies of Heavy Metals

Adsorption of Cu and Cr were carried out for all the samples under batch condition. The adsorption experiments were carried out under various process conditions for optimization such as pH, dosage, concentration, and time.
To study the kinetics and adsorption isotherms, the concentration of the $K_2Cr_2O_7$ solution was varied (10ppm,100ppm,200ppm,1000ppm). Along with it the samples were taken out at different time intervals (1min, 5min, 10min, 15min, 30min, 1h, 3h, 6h and 24h) to study the Cr concentration using ICP-OES.

The amount of adsorption at equilibrium q_e (mg/g) was calculated by:

$$q_e=(Co-Ce)V/W$$

where Co and Ce are the initial and equilibrium concentration (mg/L) of the metal ions respectively. V is the volume of the solution (L) and W is the mass of dry adsorbent used (g).
The amount of adsorption at time t, q_t (mg/g) was calculated by:

$$q_t=(Co-Ct)V/W$$

where Co is the initial concentration(mg/L) and C_t concentration (mg/L) of the dye at any time t. V is the volume of the solution (L) and W is the mass of dry adsorbent used (g).

3.3.3. Heavy metal concentration determination using ICP-OES

Prior to ICP-OES analysis Metal ion solutions, obtained after adsorption were diluted to 10ppm concentration based on the initial concentration of stock solution (i.e., samples obtained after adsorption of 100ppm metal ion solution were all diluted to a 1:10 ratio, samples obtained from 200ppm solution were all diluted to 1:20 ratio; 1000 ppm to 1:100 ratio), standards for detection of both Copper and Chromium ions were obtained by dilution of Perkin Elmer Multi Element Standard to 0.1, 0.5 and 1ppm concentration, 5% nitric acid was taken as blank, and the same would be used as intermediate cleaning buffer.

All liquids involved in the process were passed through 20-micron syringe filters, and stored in sealed containers before analysis. During the operation of the ICP equipment, all measurements were taken as triplicates, and a blank flow of two minutes was allowed in between consecutive runs.

4. INSTRUMENTS AND APPARATUS:

4.1.BET Surface Area Analyzer



Figure 2: BET by Quantachrome Autosorb

Brunauer-Emmett-Teller (BET) surface area analysis is the multi-point measurement of an analyte's specific surface area (m2/g) through gas

adsorption analysis, where an inert gas such as nitrogen is continuously flowed over a solid sample, or the solid sample is suspended in a defined gaseous volume.

Small gas molecules adsorb to the solid substrate and its porous structures due to weak van der Waals forces, forming a monolayer of adsorbed gas. This monomolecular layer, and the rate of adsorption, can be used to calculate the specific surface area of a solid sample and its porous geometry, informing studies into the reactivity and bioavailability of pharmaceutical products.

The BET is a method for determining the surface area of solid or porous materials. This is a basic technique used across several disciplines, especially in chemistry, material science and nanotechnology.

How does it work?

Adsorption : Nitrogen gas is passed over a solid substance or matrix which causes the particle to absorb it.

Isotherm: Quantity of a gas adsorbed on the other side is monitored by taking different pressure with respect to temperature forming an Adsorption Isotherm.

BET Equation: It is a mathematical form which models the multilayered adsorption of analytical data for fitting in relation to BET Method.

Calculation of Surface Area: the BET equation can be used for determining the specific surface area.

Advantage of BET:-

The advantages of BET analysis include its ability to provide quantitative data on surface area and porosity, its non-destructive nature, and its versatility in analysing a wide range of materials. It is a fundamental technique for understanding the textural properties of materials.

BET Equation:

The BET equation is a mathematical model that describes the adsorption of gas molecules onto a solid surface. It's a fundamental equation in BET analysis and provides a way to calculate the specific surface area of a material.

$$\mathbf{(P/V)\ (P_o - P) = 1/V_mC + (C - 1)/V_mC * P}$$

Where:

P: Pressure of the gas

V: Volume of gas adsorbed at pressure P

P_0: Saturation pressure of the gas

V_m: Monolayer capacity (the volume of gas required to form a single layer on the surface) C: A constant related to the enthalpy of adsorption

By plotting the left-hand side of the equation against P/P_0, a straight line is obtained. The slope and

intercept of this line can be used to determine V_m and C. Once V_m is known, the specific surface area can be calculated using the following equation:

Surface area = V_m * N_a * σ / ρ

Where:

N_a: Avogadro's number

σ: Cross-sectional area of the adsorbed gas molecule

ρ: Density of the solid material

4.2.Thermogravimetric analyser



Figure 3: TGA by PerkinElmer

Thermogravimetric analysis (TGA) is conducted on an instrument referred to as a thermogravimetric analyser. A thermogravimetric analyser continuously measures mass while the temperature of a sample is changed over time. Mass, temperature, and time are considered base measurements in thermogravimetric analysis while many additional measures may be derived from these three base measurements.

A typical thermogravimetric analyser consists of a precision balance with a sample pan located inside a furnace with a programmable control temperature. The temperature is generally increased at constant rate (or for some applications the temperature is controlled for a constant mass loss) to incur a thermal reaction. The thermal reaction may occur under a variety of atmospheres including: ambient air, vacuum, inert gas, oxidizing/reducing gases, corrosive gases, carburizing gases, vapours of liquids or "self-generated atmosphere"; as well as a variety of pressures including: a high vacuum, high pressure, constant pressure, or a controlled pressure.

Thermogravimetric analysis (TGA) is conducted on an instrument referred to as a thermogravimetric analyser. A thermogravimetric analyser continuously measures mass while the temperature of a sample is changed over time. Mass, temperature, and time are considered base measurements in thermogravimetric analysis while many additional measures may be derived from these three base measurements.

A typical thermogravimetric analyser consists of a precision balance with a sample pan located inside a furnace with a programmable control temperature. The temperature is generally increased at constant rate (or for some applications the temperature is controlled for a constant mass loss) to incur a thermal reaction. The thermal reaction may occur under a variety of atmospheres including: ambient air, vacuum, inert gas, oxidizing/reducing gases, corrosive gases, carburizing gases, vapors of liquids or "self-generated atmosphere"; as well as a variety of pressures including: a high vacuum, high pressure, constant pressure, or a controlled pressure.

The thermogravimetric data collected from a thermal reaction is compiled into a plot of mass or percentage of initial mass on the y axis versus either temperature or time on the x-axis. This plot, which is often smoothed, is referred to as a TGA curve. The first derivative of the TGA curve (the DTG curve) may be plotted to determine inflection points useful for in-depth interpretations as well as differential thermal analysis.

A TGA can be used for materials characterization through analysis of characteristic decomposition patterns. It is an especially useful technique for the study of polymeric materials, including thermoplastics, thermosets, elastomers, composites, plastic films, fibres, coatings, paints, and fuels.

Types of TGA

There are three types of thermogravimetry:

Isothermal or static thermogravimetry: In this technique, the sample weight is recorded as a function of time at a constant temperature.

Quasistatic thermogravimetry: In this technique, the sample temperature is raised in sequential steps separated by isothermal intervals, during which the sample mass reaches stability before the start of the next temperature ramp.

Dynamic thermogravimetry: In this technique, the sample is heated in an environment whose temperature is changed in a linear manner.

Advantages of TGA:

Sensitivity: Can detect small changes in mass.

Versatility: Can be used to study a wide range of materials.

Quantitative Analysis: Can be used to determine the amount of specific components in a sample.

4.3. FTIR (Fourier-Transform Infrared Spectroscopy



Figure 4: FT/IR-4700 by JASCO

The goal of absorption spectroscopy techniques (FTIR, ultraviolet-visible ("UV-vis") spectroscopy, etc.) is to measure how much light a sample absorbs at each wavelength. The most straightforward way to do this, the "dispersive spectroscopy" technique, is to shine a monochromatic light beam at a sample, measure how much of the light is absorbed, and repeat for each different wavelength. (This is how some UV–vis spectrometers work, for example.)

Fourier-transform spectroscopy is a less intuitive way to obtain the same information. Rather than shining a monochromatic beam of light (a beam composed of only a single wavelength) at the sample, this technique shines a beam containing many frequencies of light at once and measures how much of that beam is absorbed by the sample. Next, the beam is modified to contain a different

combination of frequencies, giving a second data point. This process is rapidly repeated many times over a short time span. Afterwards, a computer takes all this data and works backward to infer what the absorption is at each wavelength.

The beam described above is generated by starting with a broadband light source one containing the full spectrum of wavelengths to be measured. The light shines into a Michelson interferometer a certain configuration of mirrors, one of which is moved by a motor. As this mirror moves, each wavelength of light in the beam is periodically blocked, transmitted, blocked, transmitted, by the interferometer, due to wave interference.

Different wavelengths are modulated at different rates, so that at each moment or mirror position the beam coming out of the interferometer has a different spectrum.

As mentioned, computer processing is required to turn the raw data (light absorption for each mirror position) into the desired result (light absorption for each wavelength). The processing required turns out to be a common algorithm called the Fourier transform. The Fourier transform converts one domain (in this case displacement of the mirror in cm) into its inverse domain (wavenumbers in cm−1). The raw data is called an "interferogram".

Advantages of FTIR:

Comprehensive Analysis: Provides both qualitative and quantitative information about the sample.

Versatility: Can be used to analyse a wide range of materials, including solids, liquids, and gases.

Sensitivity: Can detect trace elements and compounds.

Non-destructive: Does not require the destruction of the sample.

Beer-Lambert Law:

The Beer-Lambert law relates the absorbance of a sample to its concentration and path length. It is used to quantify the concentration of a known analyte in a sample.

$A = \varepsilon bc$

Where:

A is the absorbance

ε is the molar absorptivity

b is the path length

c is the concentration

Fourier Transform:

The Fourier transform is a mathematical operation used to convert the interferogram (time-domain signal) into a frequency-domain spectrum. The Fourier transform equation is:

$F(\omega) = \int f(t) * e^{(-i\omega t)} dt$

Where:

$F(\omega)$ is the Fourier transform $f(t)$ is the time-domain signal ω is the angular frequency.

How FTIR Works:

FTIR Analysis: The sample is first analysed using FTIR to identify the chemical functional groups present.

Data Correlation: The FTIR data is correlated to determine the specific elements and compounds present in the sample.

4.4.Inductively Coupled Plasma Optical Emission Spectroscopy (ICP-OES)

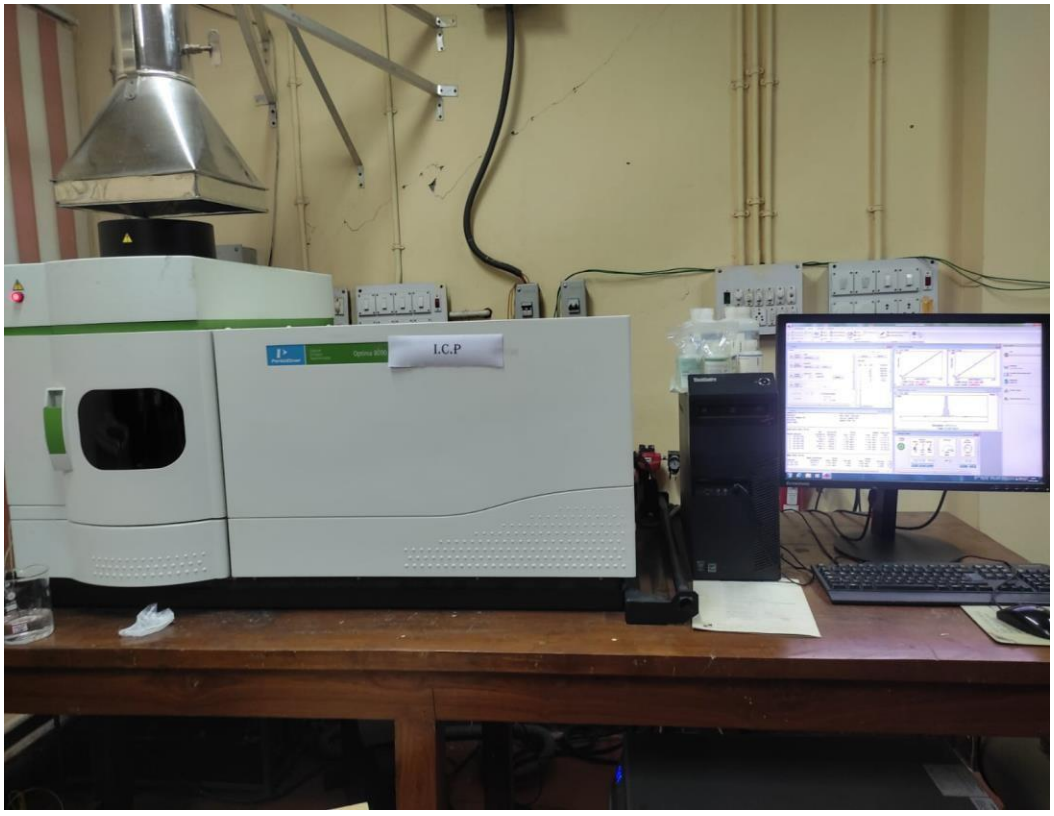


Figure 5: ICP by PerkinElmer

ICP-OES is a powerful analytical technique used to determine the elemental composition of samples. It's particularly effective for analysing trace elements at very low concentrations.

How ICP-OES Works:

Sample Introduction: The sample is introduced into a nebulizer, which converts it into a fine aerosol.

Plasma Formation: The aerosol is carried into an inductively coupled plasma (ICP), a high- temperature plasma generated by an electric current passing through a coil of wire.

Excitation: The atoms and ions in the sample are excited by the high temperature of the plasma.

Emission: When the excited atoms and ions return to their ground state, they emit light at specific wavelengths.

Spectral Analysis: The emitted light is analysed using a spectrometer to determine the elemental composition of the sample based on the wavelengths of the emitted lines

Advantages of ICP-OES:

Sensitivity: Can detect elements at very low concentrations.

Multi-element Analysis: Can simultaneously analyse multiple elements in a single sample.

Wide Dynamic Range: Can measure elements over a wide range of concentrations.

Accuracy: Provides accurate and precise results.

5. Novelty of Work

PEI /CNC-PVA (S6) and PEI /CNC (S4) aerogels represent a novel and effective material for the removal of heavy metals from wastewater. Their novelty stems from several key factors:

- **High Specific Surface Area:** Compared to other cellulose based aerogel, which are quite costly because of energy extensive drying techniques, this freeze-dried aerogel has comparatively higher specific surface area.
- **Functionalization with PEI:** Polyethyleneimine (PEI) is a cationic polymer rich in amino groups. These amino groups can chelate with heavy metal ions (such as Pb^{2+}, Cd^{2+}, Hg^{2+}, etc.), enhancing the aerogel's affinity for heavy metals.
- **lower rate of degradation:** It has very low degradation rate making it reuseable and regeneratable.
- **High Removal Efficiency:** It gives more than 90% adsorption efficiency towards selective metal ions.
- **Lightweight and Mechanically Robust:** Surface modification with $NaIO_4$ and incorporating binding agent like PVA has massively aided the aerogel to be mechanically stable compared to the others.

6. Results

6.1. Removal of Cr (VI) ion using surface modified aerogels

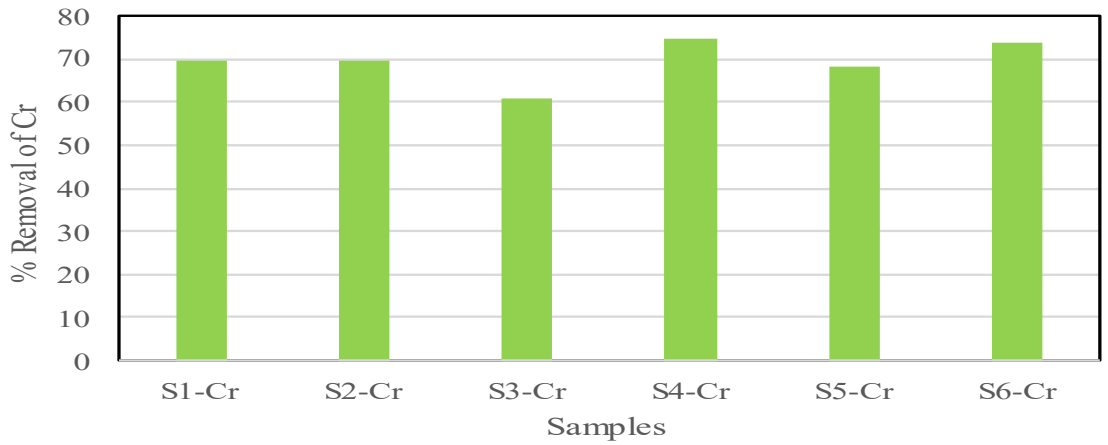


Figure 6: Removal of Cr

Adsorption experiments were carried out using 100 mL of aqueous $K_2Cr_2O_7$ solution of pH 7 of initial concentrations of 10 ppm in a series of 25 mL Test tubes, maintained at temperature of 25 °C. The test tubes were shaken at 120 rpm for an equilibrium time of 24 h in an incubator shaker. 1g/L of adsorbent dosage of each sample was taken for the study.

All the samples exhibited high Cr (VI) adsorption capacity (greater than 60% removal) as depicted in Figure 6 As per the ICP-OES data, S4 has shown the highest removal capacity of ~74% for Cr (VI) ion. The possible reason could be the abundance of the -NH_2 group present in the aerogel surface which is cationic in nature and the ionic attraction between the metal ions and the surface of the aerogel causing high adsorption efficiency. The 3D porous structure also improved the Cr (VI) sorption on S4 and S6 surfaces through physical interactions.

6.2.Removal of Cu (II) ion using surface modified aerogels

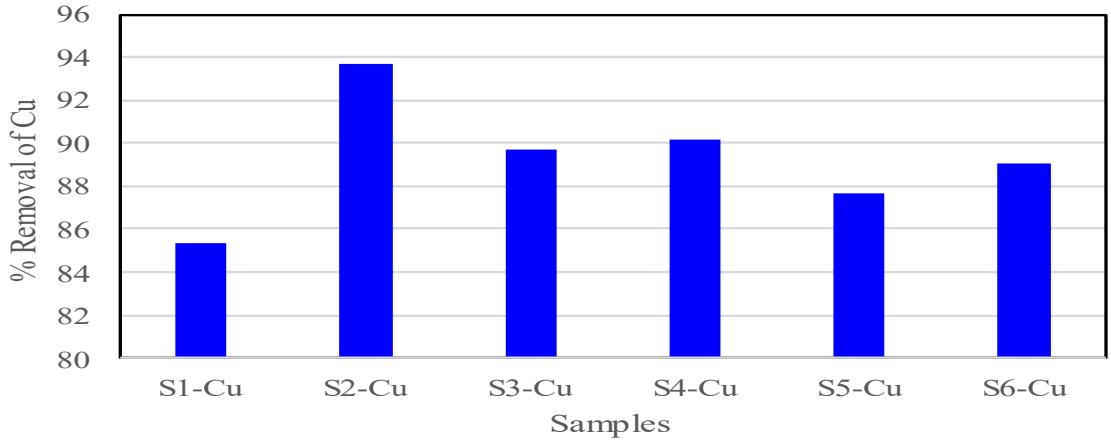


Figure 7: Removal of Cu

In Cu (II) ion adsorption the S2 aerogel has shown the highest adsorption capacity of ~93%. An abundance of the -OH group incorporated through PEG helped in the interionic attraction. Also, the addition of $NaIO_4$ provided more anionic groups like -COOH on its surface. Also, ICP data indicates that the $-NH_2$ groups, together with -OH also participated in the adsorption of Cu (II) in the case of S4 and S6 aerogels. In terms of physical stability, all the amine-modified aerogels (S4, S5, S6) performed better.

6.3. Effect of pH

The solution pH is one of the important parameters that govern adsorption processes. The pH of the solution not only affects the surface charge of the adsorbents, but also alters the degree of ionization of different pollutants. Variation in pH affects the adsorptive process through dissociation of functional groups on the adsorbent surface-active sites resulting to a shift in reaction kinetics and equilibrium characteristics of adsorption processes.

6.3.1. Effect of pH in Cu (II) adsorption

The effect of pH on the adsorption of Cu (II) is shown in the below Fig. It was evident that ion adsorption increased slightly over the pH range of 2–6 while a drastic increase was observed at pH 8 and pH 10. Lower adsorption efficiency of Cu (II)ion at lower pH was due to the presence of excess H+ ions competing with the cation groups on the solution for adsorption sites. The sharp increase after pH 8 can be attributed to the strong electrostatic attraction between the metal ion and the aerogels surface functionalization groups. At pH 8 S4 has shown the highest adsorption capacity for Cu (II) ion. The change in adsorption in this region (pH6-12) is probably due to the sharp variation in magnitude of the charge carried by the functionalization groups of the adsorbent. Increasing solution pH increases the number of hydroxyl groups thereby increasing the number of negatively charge sites. At higher pH, the surface functional groups on the activated carbon were deprotonated resulting in a decrease in surface charge density thus enhancing the attraction between metal ion and adsorbent surface. Since the highest adsorption capacity was observed at pH 10, it was taken as the optimum pH for all further experiments in the study.

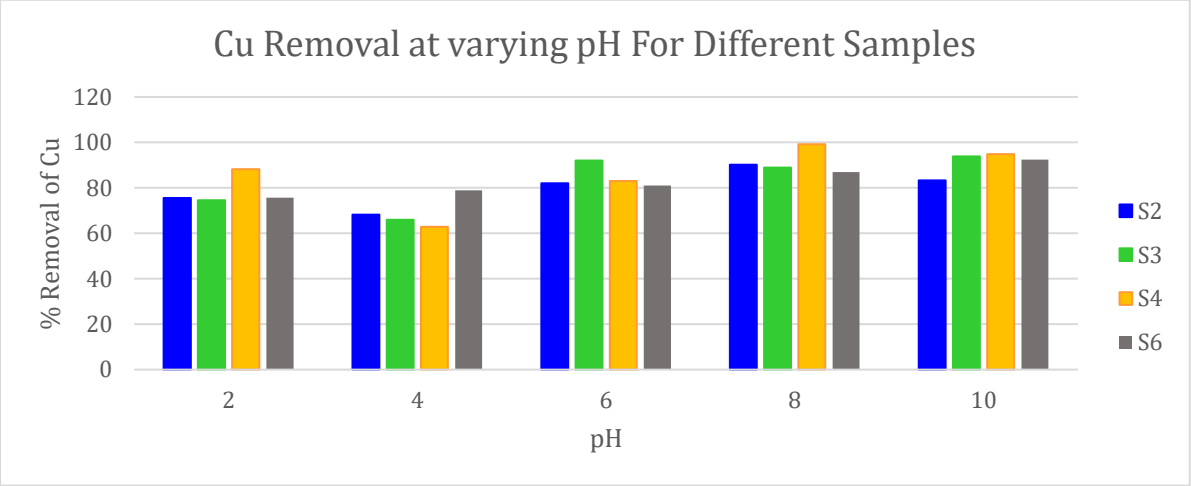


Figure 8: pH variation for Cu

6.3.2. Effect of pH in Cr (VI) adsorption

In the figure mentioned below the adsorption of Cr (VI) ion was studied. It is evident from the data that adsorption was slightly decreased over a pH range of 2-8. A drastic decrease in adsorption capacity was witnessed when the pH value increased from 6 to 8. The amine groups present in the aerogel surface of S4 were positively charged at pH below 8 and negatively charged at pH>6. It might be explained that in a strong acidic environment, the numerous active groups (NH_3^+) on the surface of the aerogel would cause strong electrostatic attraction with negatively charged Cr (VI) species ($Cr_2O_7^{2-}$). As pH increased, the deprotonation of the surface of the aerogels led the free groups (–COOH, –OH, and $–NH_2$) to interact with the metal ions, due to that the electrostatic repulsive force was generated between Cr (VI) species and aerogels during this stage. From the ICP data, the pH condition of 6 was seen optimal for the adsorption of Cr (VI) by S4 aerogel.

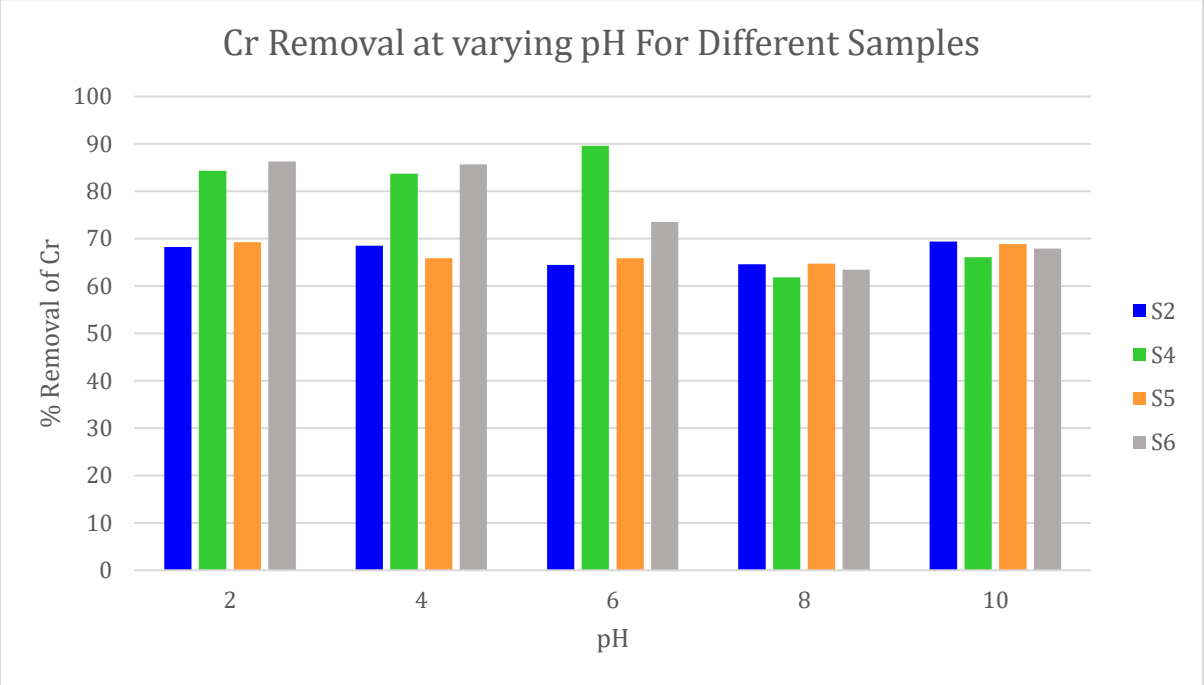


Figure 9: pH variation for Cr

6.4. Effect of adsorbent dosage

Adsorbent dosage determines the capacity of an adsorbent for a given initial concentration of the adsorbate. An increase in dosage increased the percentage of ion adsorption while a decrease in the amount adsorbed per unit mass of adsorbent. The increase in ion adsorbed was attributed to an increase in the surface area of the selected aerogels and the availability of more adsorption sites. The increase in adsorbent dosage while the decrease in unit adsorption was due to the adsorption sites remaining unsaturated during the adsorption process.

6.4.1. Effect of adsorbent dosage for Cr (VI)adsorption

For adsorbent dosage optimization, the optimum solution pH and the most efficient adsorbent were utilized using varying dosages. With the increase in adsorbent dosage, the solid-to-liquid ratio increased. The adsorption rate of Cr (VI) was enhanced with a rise in its dosage until 1g/l, further increases in dosage affect the removal efficiency negatively. Similarly, the improved Cr (VI) uptake was observed with a rise in amine-functionalized cellulose aerogel dosage because a higher amount of aerogel brought more active functional groups which trapped more Cr (VI) from the aqueous solution. In this case, 1g/L was the optimum adsorbent dosage as there was a decrease in Cr removal efficiency for 2g/l adsorbent dosage.

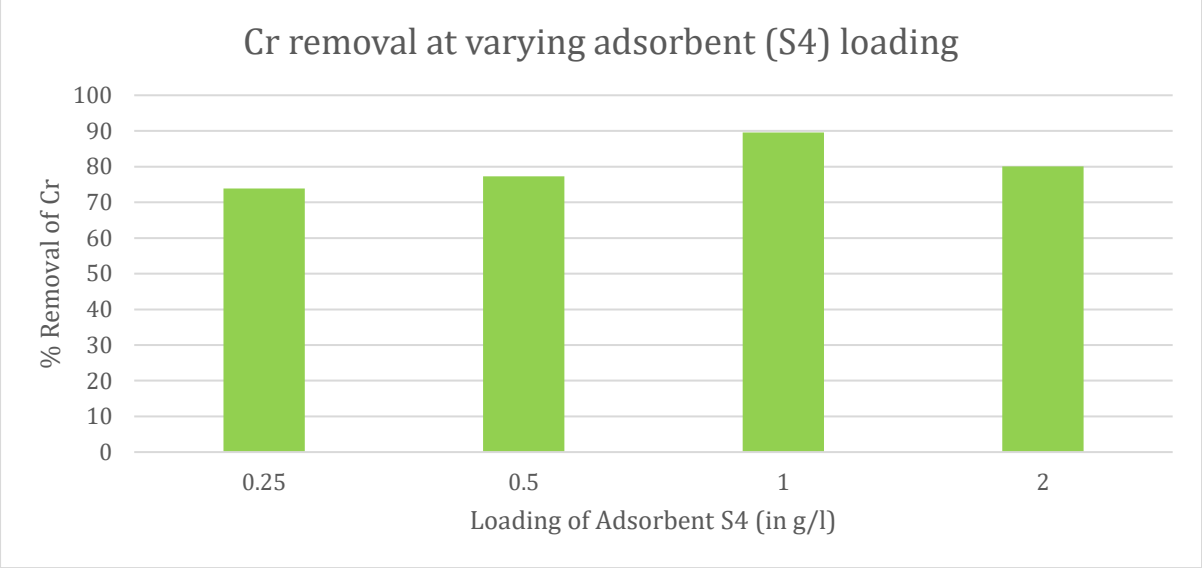


Figure 10: Dosage variance for Cr

6.4.2. Effect of adsorbent dosage for Cu (II)adsorption

For optimization of dosage amount, the optimum pH of 10 and the best aerogel S6 were selected with varying dosages. With increase in adsorbent dosage, the solid-to-liquid ratio increased. The adsorption rate of Cu (II) enhanced with a rise in its dosage. Most of the functionalization sites on the aerogel surface remain unsaturated resulting in less adsorption of Cu ions. Similarly, the improved Cu (II) uptake was observed with a rise in -OH functionalized cellulose aerogel dosage because a higher amount of aerogel brought more active -OH groups which trapped more Cu (II) from aqueous solution. In this case, 1g/L was the optimum adsorbent dosage as a further increase in adsorbent dosage decreased the Cu (II) uptake.

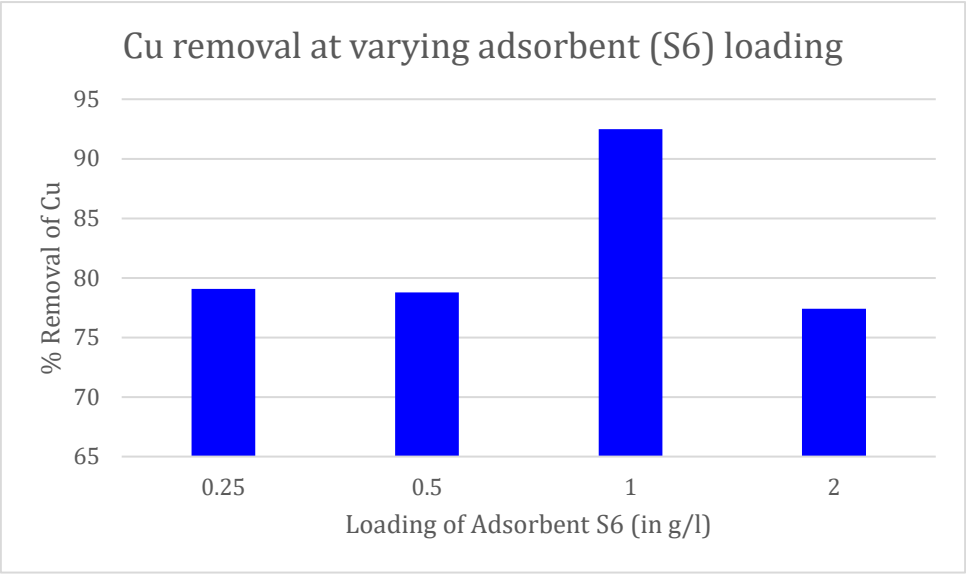


Figure 11: Dosage variance for Cu

6.5. FTIR analysis

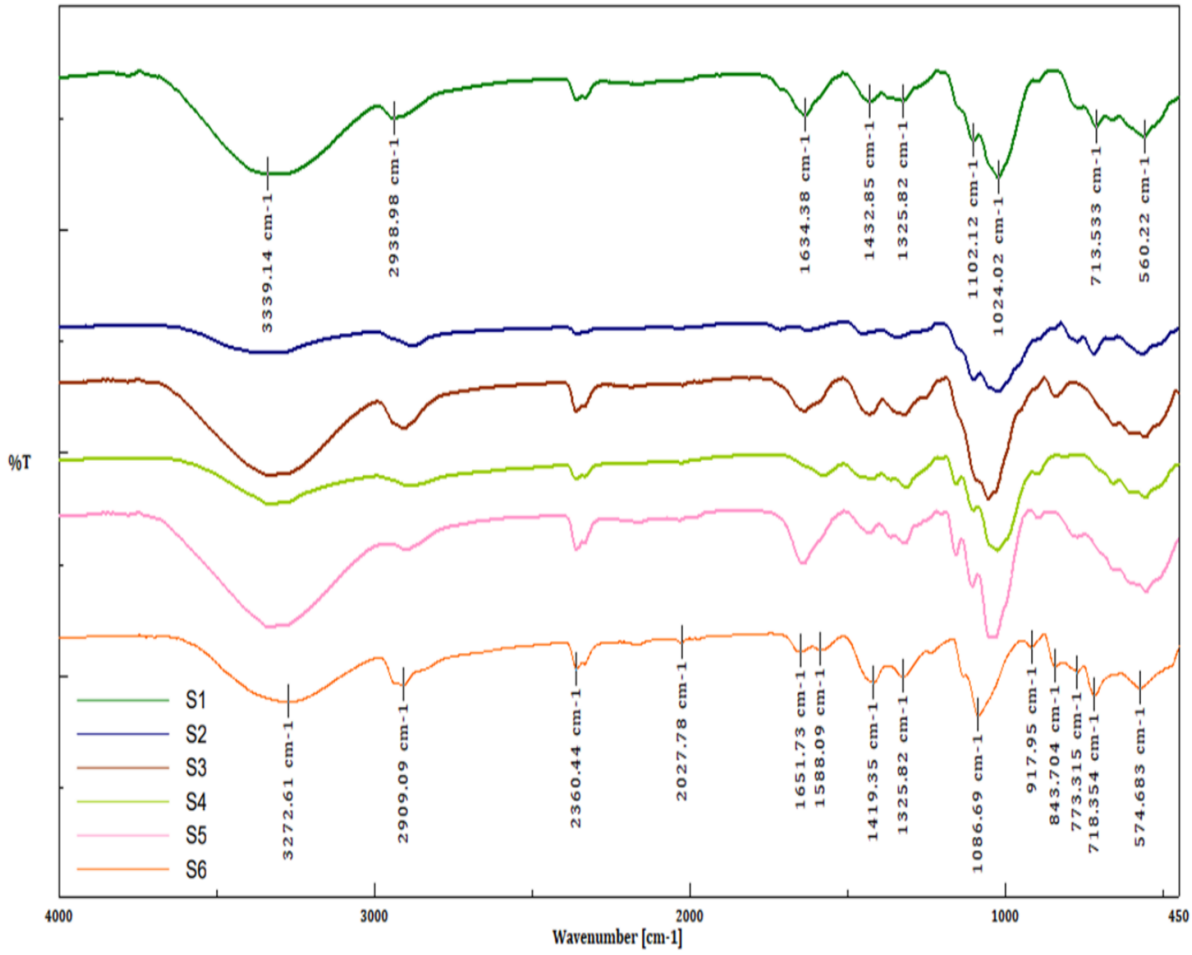


Figure 12: FTIR of Aerogels

This figure depicts the FTIR spectrum for the samples labeled as S1, S2, S3, S4, S5 and S6 in the range of 450 cm^{-1} to 4000 cm^{-1}. The broad band from 3000cm^{-1} to 3550cm^{-1} corresponds to the stretching vibrations of the hydroxyl O-H groups which are present in all the samples. Strong characteristic bands of CNC are observed at 3339.14, 2938.98, and 1102.12 cm^{-1} , which correspond to O-H stretching, asymmetric stretching of the C-H groups of CH_2, and C-O-C asymmetric stretching vibrations, respectively. Also, the band at 1024 cm^{-1} is assigned to a C-O vibration of a primary alcohol. After modification of the CNC with PEI and PVA(S6) new peaks appear at 1651.73 and 2909.09 cm^{-1}; these peaks are attributed to amine (-NH2) groups and a symmetric CH2 stretching vibration, respectively. Because PEI contains numerous amine groups connected with alkyl chains, modification of the CNC aerogel with PEI led to changes in its FTIR spectrum. The deep strong peak around 1650 cm^{-1} in S5 assures the C=O stretching of secondary amide which is due to the addition of PEI.A new absorption band located at approximately 1528cm^{-1} was observed for N-H bending of amine group in case of S6.

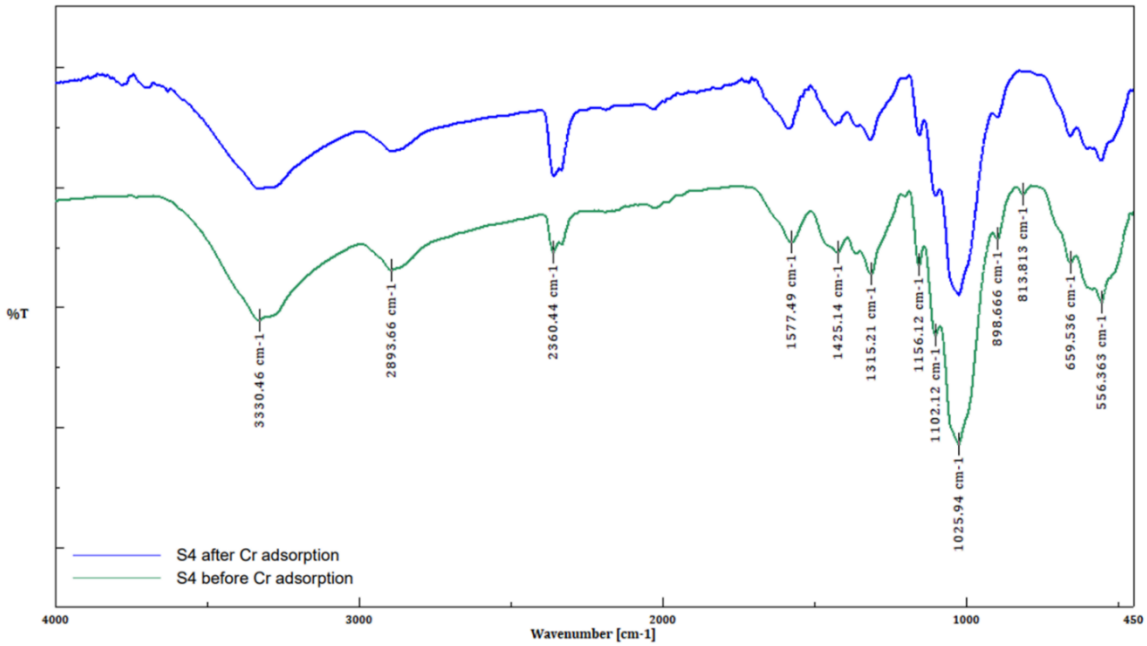


Figure 13: Cr adsorption

A convoluted peak at 2360 cm^{-1} which refers to O=C=O stretching of $CO_{2\ has}$ broadened after adsorption of chromium ion by S4 aerogel. Also, a medium band peak at 813.813 cm^{-1} which refers to C=C bending of alkene has vanished which can be a possibility of new bond formation after adsorption of Cr ion.

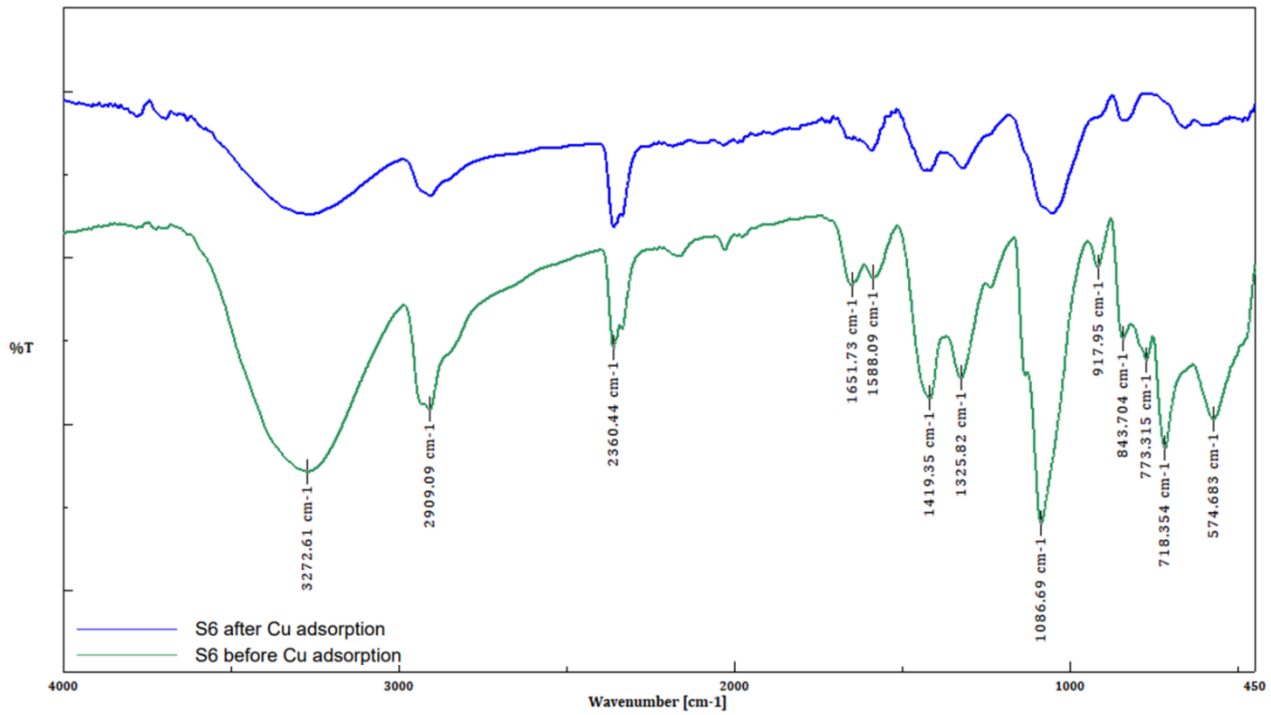


Figure 14: Cu adsorption

The sharp peak at 3272.61cm^{-1} which refers to the C-H stretching of alkyne has flattened after adsorption of Cu ion which probably converted the bond structure into O-H stretching of alcohol. The strong peak of 2909.09 cm^{-1} has also weakened showing a possible conversion of N-H stretching of amine group into O-H stretching of carboxylic acid. After adsorption of Cu ion, the peak at 1651.73 of C=N stretching of imine class has vanished which signifies either bond breaking or new bond formation.

6.6.Adsorption kinetics

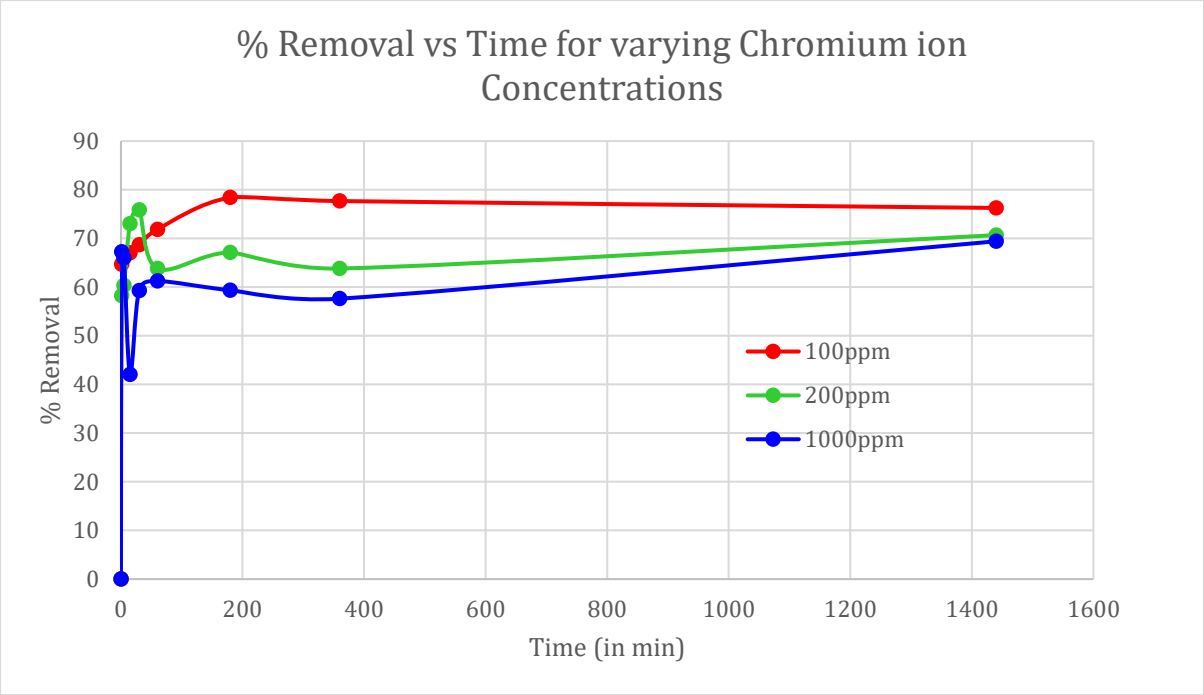


Figure 15: Kinetics Data

The effect of contact time on the S4 aerogel towards Cr (VI) ions at three initial concentrations (100,200 and 1000 mg L^{-1}) was depicted in this Figure 15. With the increase of concentration (100 to 1000 mg L^{-1}), the time needed to reach equilibrium increased from 30 to 180 min. The adsorption capacity of S4 increased rapidly and reached almost 80% in first stage, which took 30–180 min depending on concentrations of Cr (VI), then the growth trend reduced until the uptake capacity reached saturation. This result suggested that S6 could rapidly adsorb Cr (VI) attributing to the properties of the functionally modified CNC/PEI aerogel. Firstly, the porous structure of cellulose aerogel and the strong metal chelating ability of the amino group were favorable to the contraction of metal ions and active sites. Secondly, because of the large molecular weight of PEI, the active amino group was only modified on the surface of material. As it is well known, the pseudo-first-order model was based on the assumption that the internal diffusion process primarily controls adsorption. In comparison, the pseudo-second-order kinetic model was based on the assumption that the adsorption process is mainly controlled by the chemisorption of adsorbate molecules on active sites. The kinetic data of Cr (VI) on S4 were fitted by pseudo-first-order and pseudo-second-order rate equations, which were expressed as:

$$\ln(q_e - q_t) = \ln q_e - K_1 t$$

$$\frac{t}{q_e} = \frac{1}{K_2 q_e^2} + \frac{1}{q_e}$$

where q_e (mg g^{-1}) and q_t (mg g^{-1}) represent the amount of Cr (VI) adsorbed at equilibrium and time t, and K_1 (min^{-1}) and K_2 (g mg^{-1} min^{-1}) are pseudo first-order and pseudo-second order rate constant, respectively. The adsorption kinetic model curves were illustrated in Fig. a and b, and corresponding kinetic parameters from both models were listed in Table5. As indicated in Table5 , the adsorption of Cr (VI) ions by S4 was considerably better fitted with the pseudo-first-order kinetic model than the pseudo second-order kinetic model. The values of R^2 for the pseudo-first-order kinetic model were closest to 0.9999 for different original concentrations, and the calculated model agreed with the experimental values (Table 5). Based on the assumptions of the pseudo-first-order model, diffusive adsorption between the Cr (VI) ions and active sites of S6 was considered to be the rate controlling step in this study.

Table 5: kinetics data

Concentration C_0 (mg L^{-1})	q_e (mg g^{-1})	Pseudo-first-order		Pseudo-second-order	
		R^2	K_1	R^2	K_2
10	4.12	0.9296	0.0029	0.6003	0.0558
100	76.26	0.9732	0.0034	0.4049	0.0014
200	141.36	0.9939	0.004	0.6169	0.0011
1000	694.1	0.8014	0.0045	0.0791	0.002

For 10 ppm kinetic data

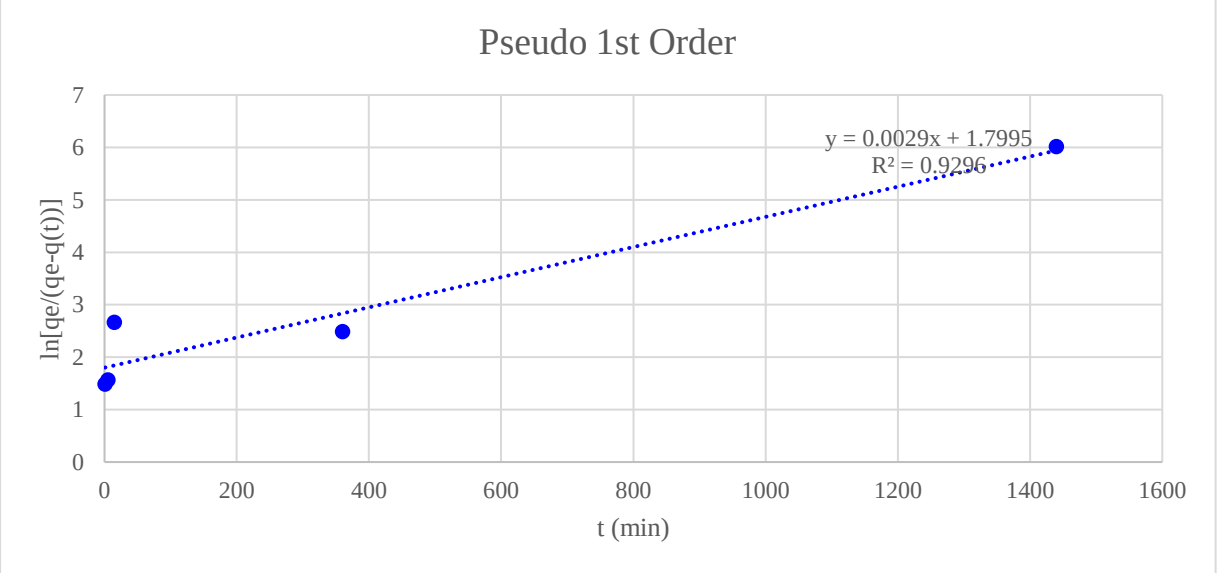


Figure 16: 10ppm kinetic data for pseudo 1st order

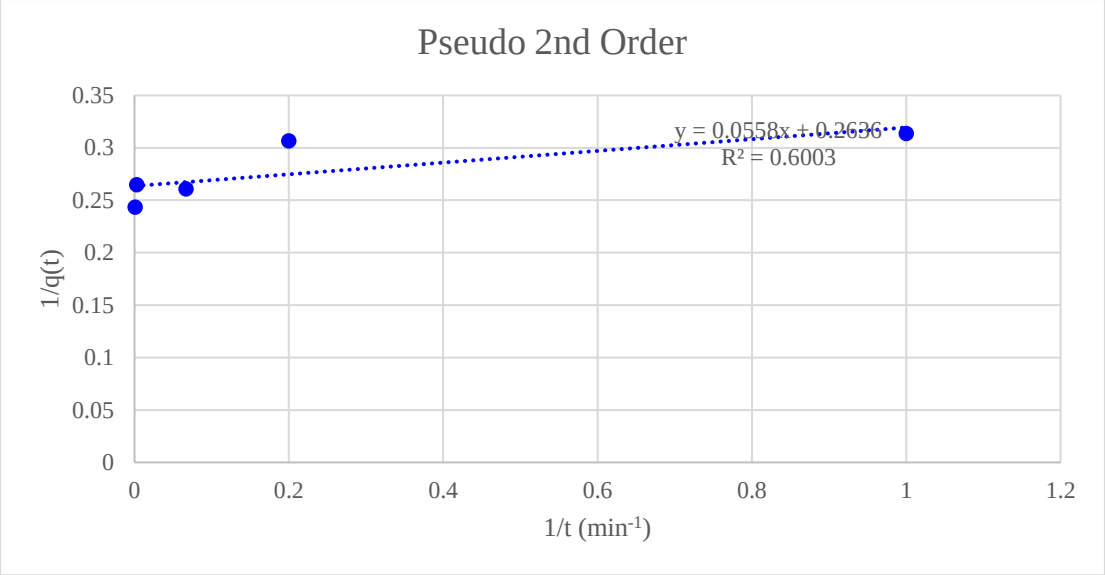


Figure 17: 10ppm kinetic data for pseudo 2nd order

For 100 ppm kinetic data

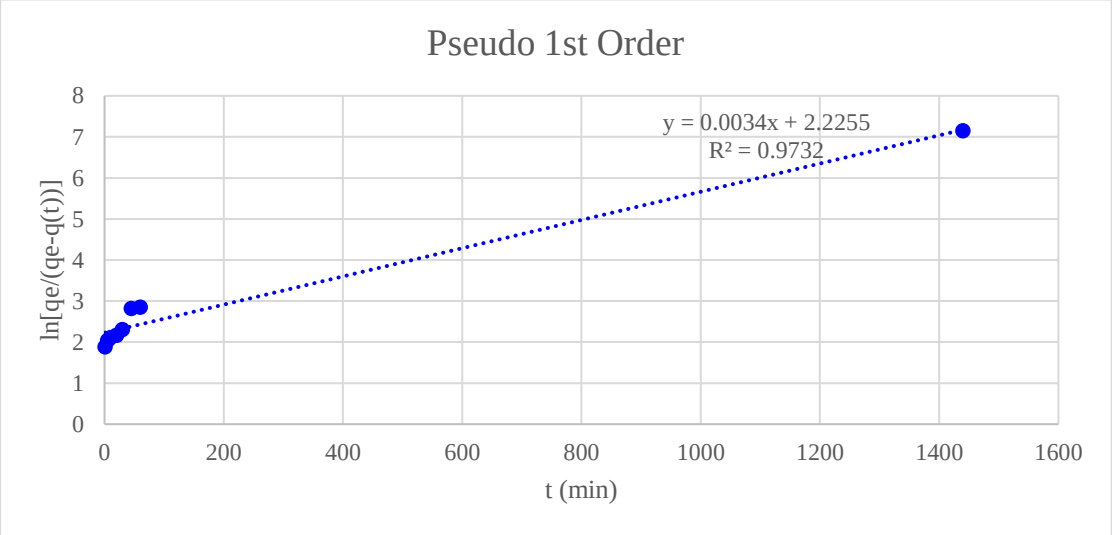


Figure 18: 100ppm kinetic data for pseudo 1st order

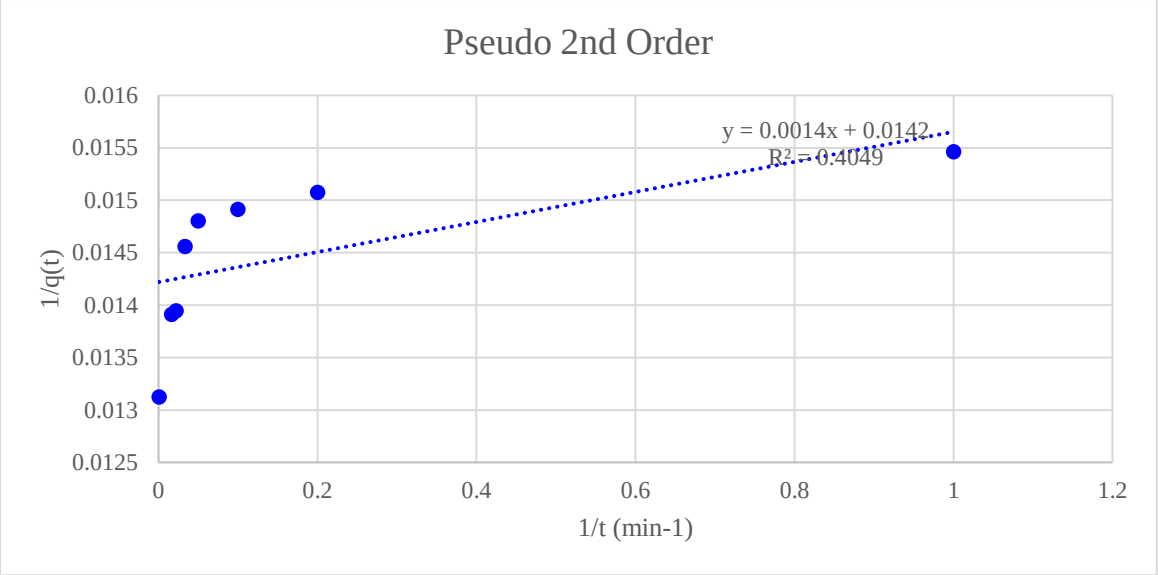


Figure 19: 100ppm kinetic data for pseudo 2nd order

For 200 ppm kinetic data

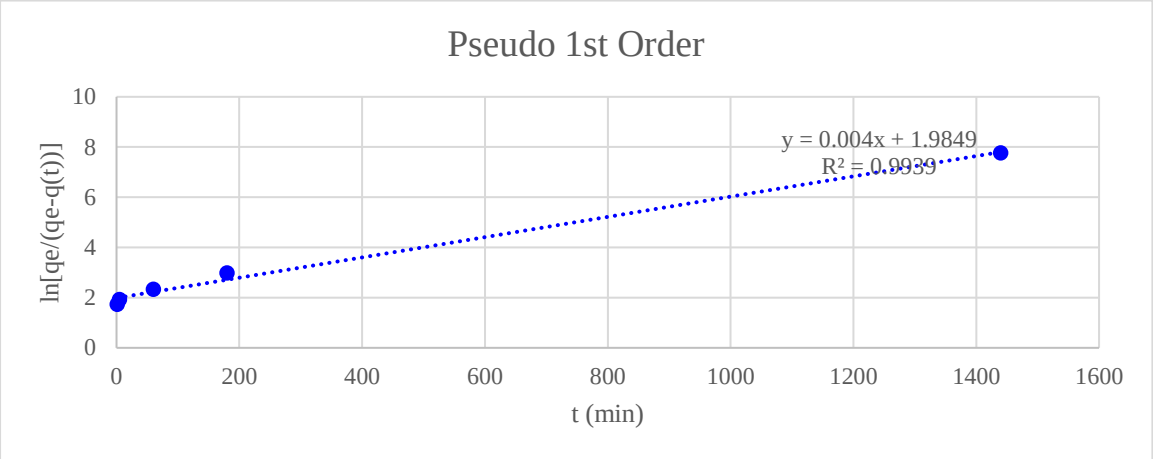


Figure 20: 200ppm kinetic data for pseudo 1st order

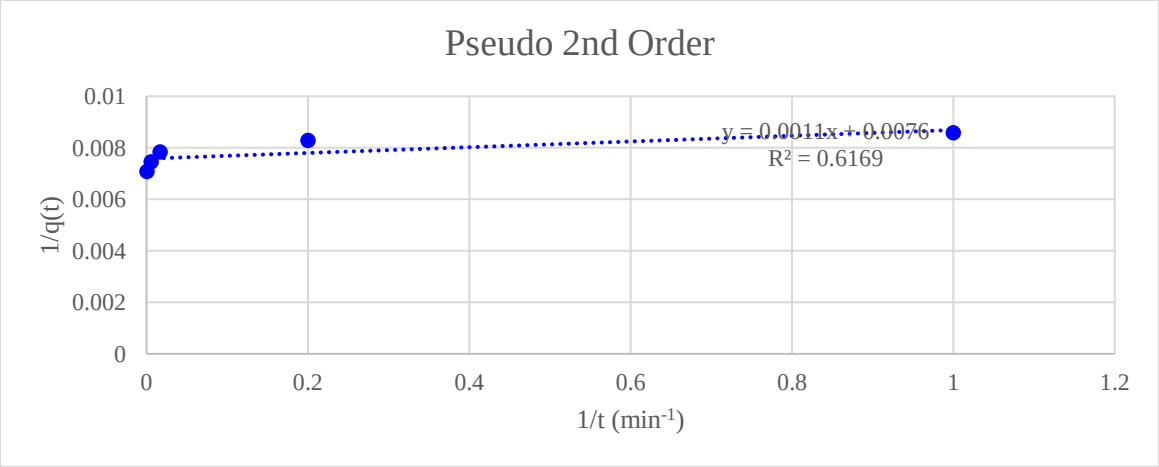


Figure 21: 200ppm kinetic data for pseudo 2nd order

For 1000ppm kinetic data

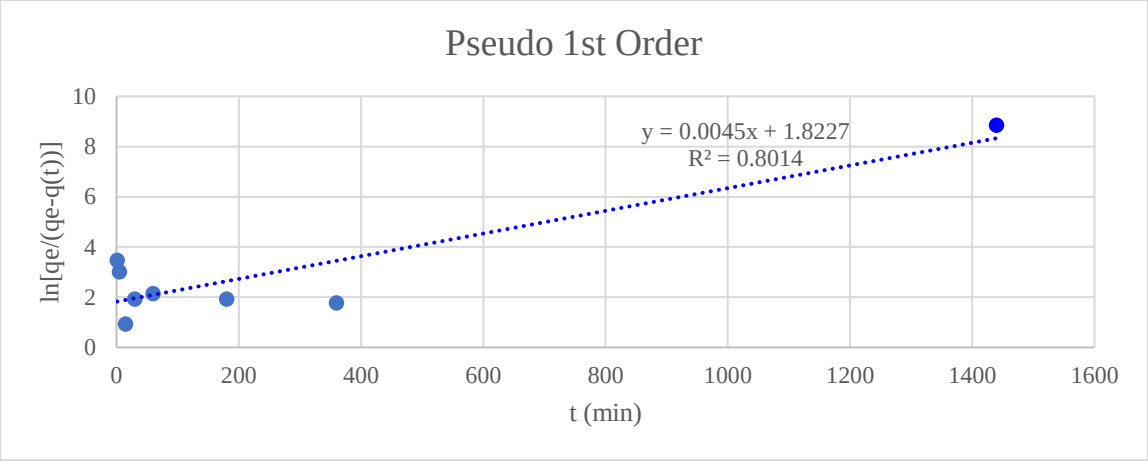


Figure 22: 1000ppm kinetic data for pseudo 1st order

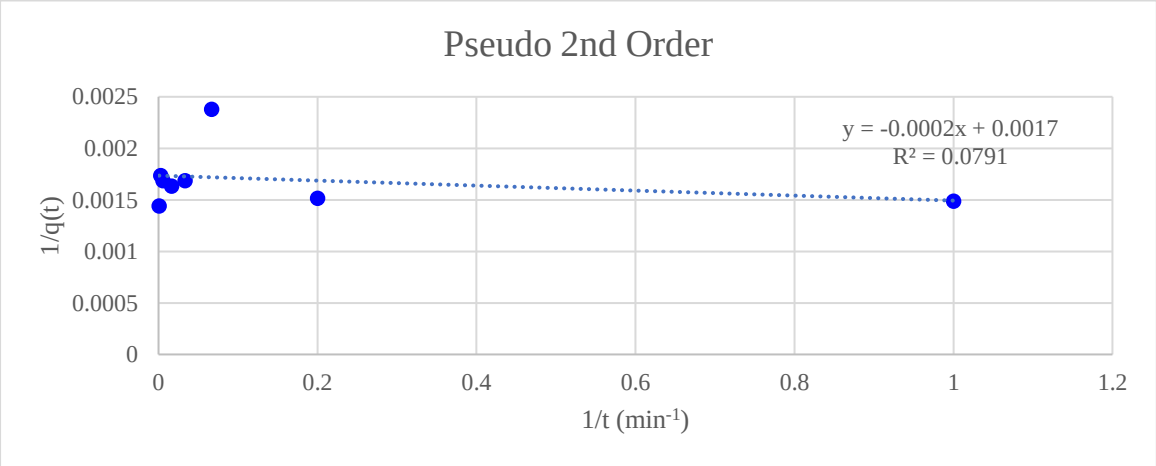


Figure 23: 1000ppm kinetic data for pseudo 2nd order

6.7. Adsorption isotherms

Adsorption isotherms are extremely important in the optimization of adsorbents, due to the fact that it not only can evaluate the efficiency of adsorbent but also reveal the interaction between adsorbate and sorbent. Accordingly, the adsorption isotherms were investigated with S6 over the initial Cr (VI) concentration range of 10–1000 mg L^{-1}at ambient temperature for 24 h. As shown in the previous kinetic data with the increase of equilibrium Cr (VI) concentration, the sorption capacities of all the aerogels increased, manifesting that the initial concentration of Cr (VI) ions played an important role in affecting the adsorption capacity. Moreover, the maximum adsorption capacity increased with increasing PEI content because of the increased number of active sites contributed by PEI molecules. In consideration, the adsorption ability and cost-effectiveness in practical applications, S4 was determined as the optimal sorbent for following experiments. Besides, when the original concentration was lower than 100 mg L^{-1}, the residual concentration of chromium after removal by S4 was inappreciable. Langmuir and Freundlich models, two famous types of isotherm models, were used to simulate the equilibrium data. Langmuir model is based on the assumption that the adsorption process is monolayer sorption on a homogeneous sorption surface and all sorption sites are almost identical. Hence, it can reach saturation. Nevertheless, the Freundlich isotherm model is used to characterize multilayer adsorption. These two models are represented as:

Langmuir:

$$q_e = \frac{q_m K_1 C_e}{1 + K_1 C_e}$$

$$R_1 = \frac{1}{1 + K_1 C_0}$$

Freundlich:

$$q_e = K_f C_e^{\frac{1}{n}}$$

where q_e and C_e are the adsorption capacity (mg g^{-1}) and Cr (VI) concentration (mg L^{-1}) at equilibrium, respectively. C_0 represents the initial concentration (mg L^{-1}) and q_m represents the maximum adsorbing capacity (mg g^{-1}). K_1 represents Langmuir constant (L mg^{-1}) related to the adsorption energy, K_f and n are related to the capacity and intensity of the adsorption, respectively, and R_1 is Langmuir constant separation factor. The non-linear adsorption isotherm curves were presented in Figure 24 and Figure 25, and related parameters of the adsorption isotherm models were summarized in Table 5. The correlation coefficient R^2 of Freundlich model of all CNC/PEI aerogels was lower than that of Langmuir model, suggesting that heterogeneous coverage of target hexavalent chromium on the surface of CNC/PEI aerogels. The correlation to the Freundlich model can support the existence of electrostatic interaction between Cr (VI) and functional groups of S4. It is worth mentioning that the correlation coefficient R^2 of Freundlich model and Langmuir model was close. To further analyze, the non-linear adsorption isotherm curves of Cr (VI), isotherm curves could fit well with Langmuir model when the concentration is low. This phenomenon may be attributed to the electrostatic attraction between protonated –NH3 + and Cr (VI) anions. If Cr (VI) concentration is low, the

surface active sites would dominate the adsorption, making the sorption process follow monolayer sorption. When the concentration is higher, the adsorption process follows multilayer adsorption. Interestingly, the adsorption isotherm of chromium onto S4 fitted better with the Langmuir model, implying a monolayer adsorption process. From the Freundlich model, it can be observed that adsorption intensity n>1, which indicates that the adsorption is favorable. Moreover, the values of R_1 were between 0 and 1, revealing the favorable adsorption of Cr (VI) by CNC/PEI-PVA aerogel, too. From the data it is evident that the S4 has a better adsorption capacity than previously reported adsorbents, indicating that S4 has a good potential in the decontamination of chromium-polluted water.

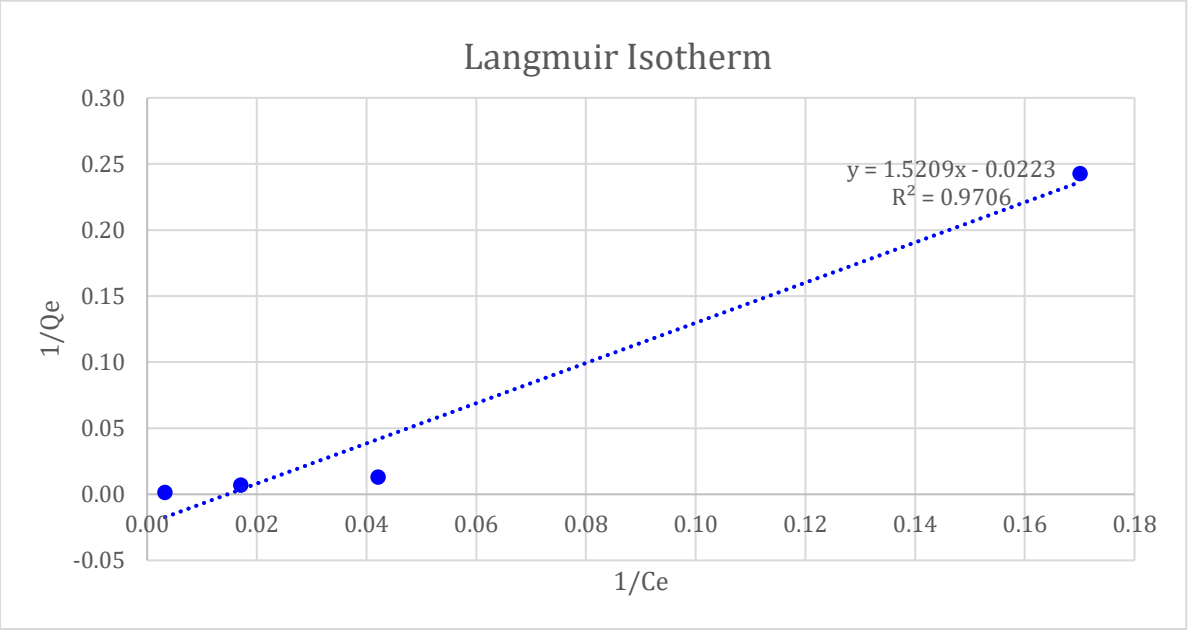


Figure 24: Langmuir Isotherm

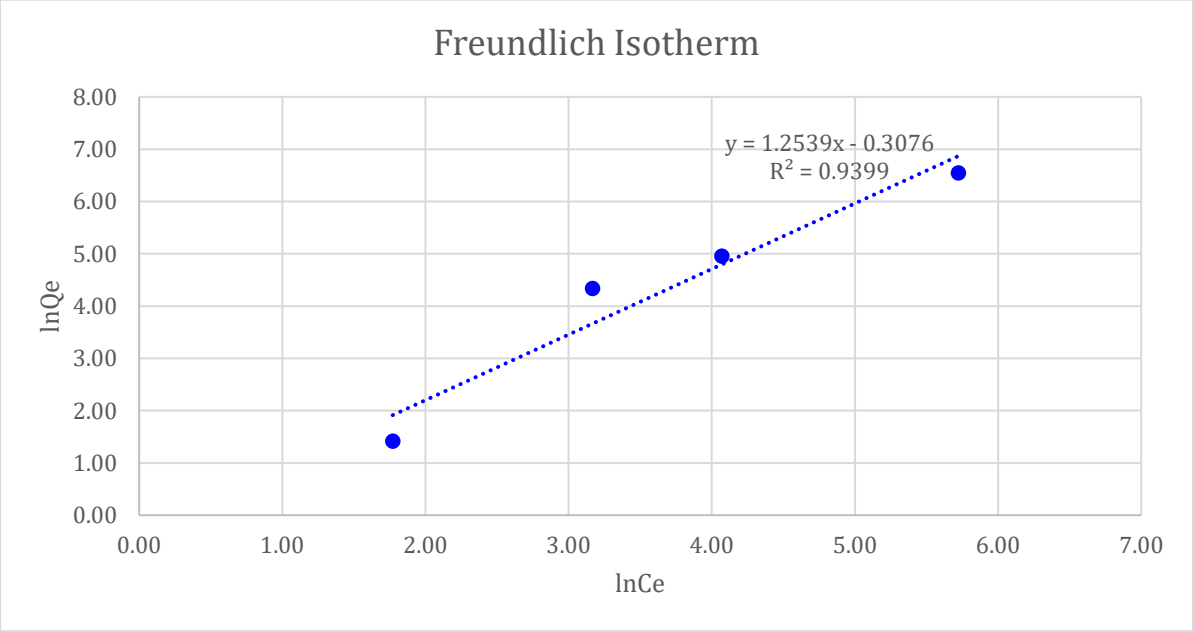


Figure 25: Freundlich Isotherm

The Dubinin–Radushkevich model :

The Dubinin–Radushkevich model is often used to estimate the characteristic porosity and the apparent free energy of adsorption. The Dubinin–Radushkevich (D–R) adsorption isotherm is represented as:

$\ln C_{ads} = \ln X_m - \beta\varepsilon^2$

where Cads is the amount of sorbate sorbed onto sorbent surface (mg/g) and X_m represents the maximum sorption capacity of sorbent (mg/g), β is constant related to sorption energy, while ε is Polanyi sorption potential which is equal to:

$\varepsilon = RT \ln (1+ 1/Ce)$

R is a gas constant in kJ mol^{-1} K^{-1}, T is the temperature in Kelvin, and Ce is the equilibrium concentration of sorbate in solution (mg/l) .The Polanyi sorption theory postulates fixed volume of sorption sites close to the sorbent surface and existence of sorption potential over these sites. Polanyi sorption potential, ε is the work required to remove a molecule to infinity from its location in the sorption space, independent of temperature. This model assumes the heterogeneity of sorption energies within this space.

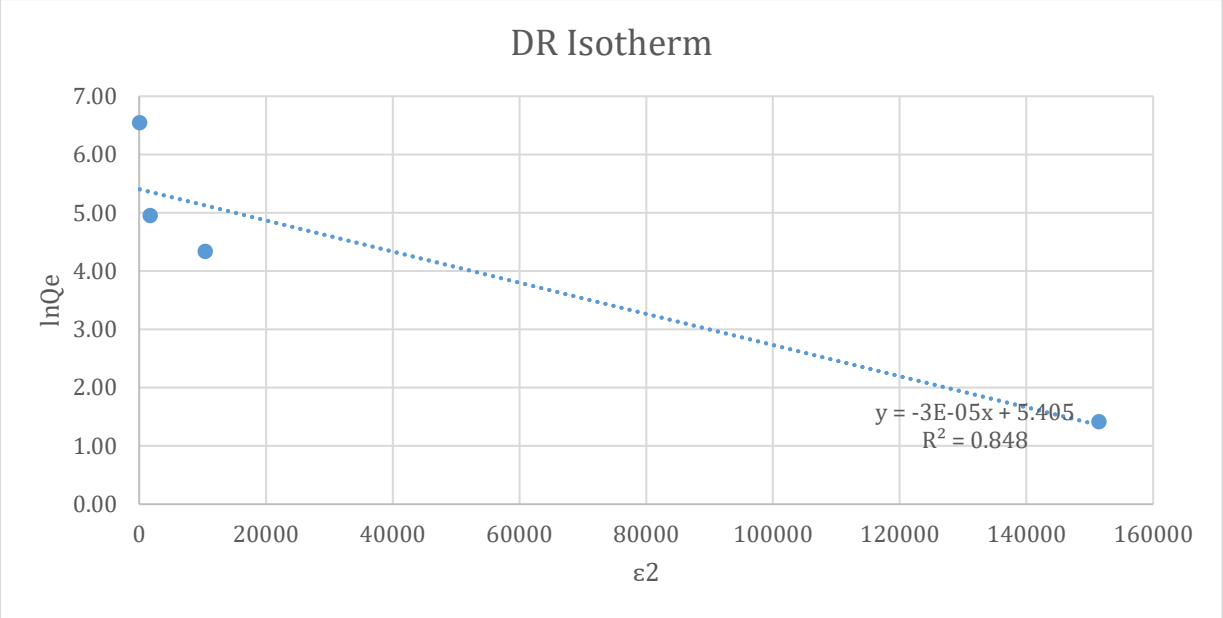


Figure 26: DR Isotherm

Temkin isotherm equation:

Temkin isotherm equation contains a factor that explicitly takes into account adsorbing species– adsorbate interactions. It assumes that: the heat of adsorption of all the molecules in the layer decreases linearly with coverage due to adsorbate–adsorbate repulsions and the adsorption is uniform distribution of maximum binding energy. In addition, it assumes that the fall in the heat of sorption is linear rather than logarithmic, as implied in the Freundlich equation. It has commonly been written as

$q_e = (RT)/b_T \log (A_T Ce)$

where $B_T = (RT)/b_T$, T is the absolute temperature in Kelvin and R is the universal gas constant, 8.314 $Jmol^{-1}$ K^{-1}. The constant b_T is related to the heat of adsorption; A_T is the equilibrium binding constant (L/g) corresponding to the maximum binding energy.

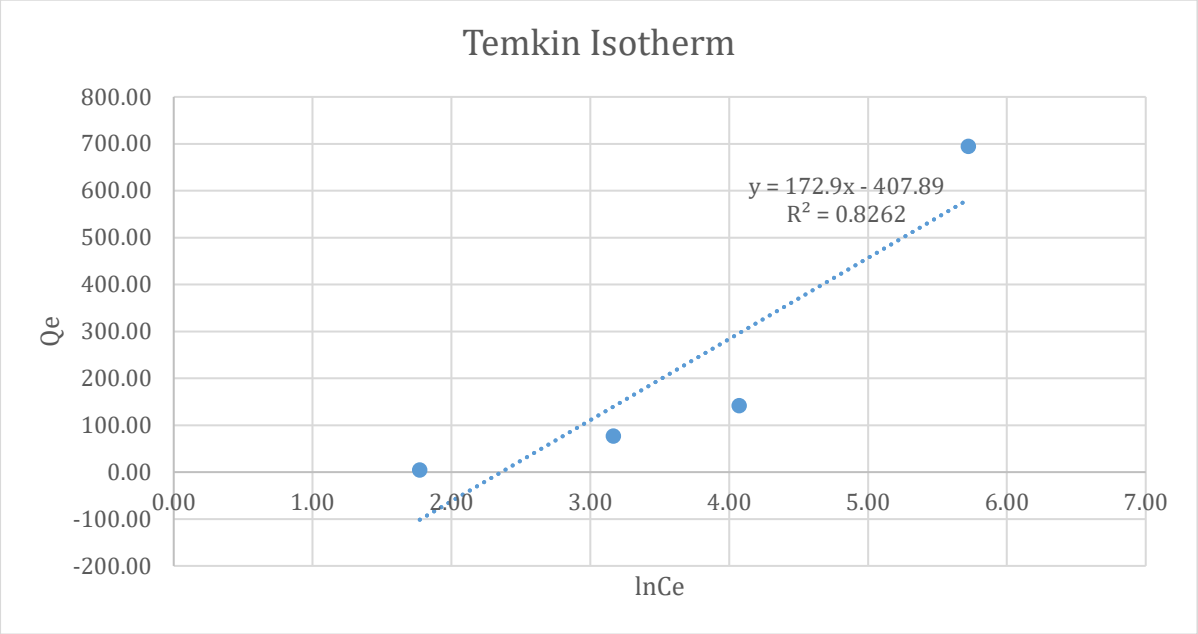


Figure 27: Temkin Isotherm

6.8. BET analysis

The relevant textural parameters of S4 and S6 calculated from nitrogen adsorption–desorption isotherms were depicted by the below Figure 28. It revealed that the BET surface area of S6(19.27 m^2 g^{-1}) was smaller than that of S4(27.7 m^2 g^{-1}). The average pore sizes of S4 and S6 were approximately 18 and 12nm, respectively. The most likely cause is that PEI molecules were grafted on CNC hydrogels and addition of PVA caused blockage on the surface of the S6 Sample. Both S4 and S6 are typical for mesoporous material. The mesopore structure is favorable for mass transfer between sorbent and hexavalent chromium.

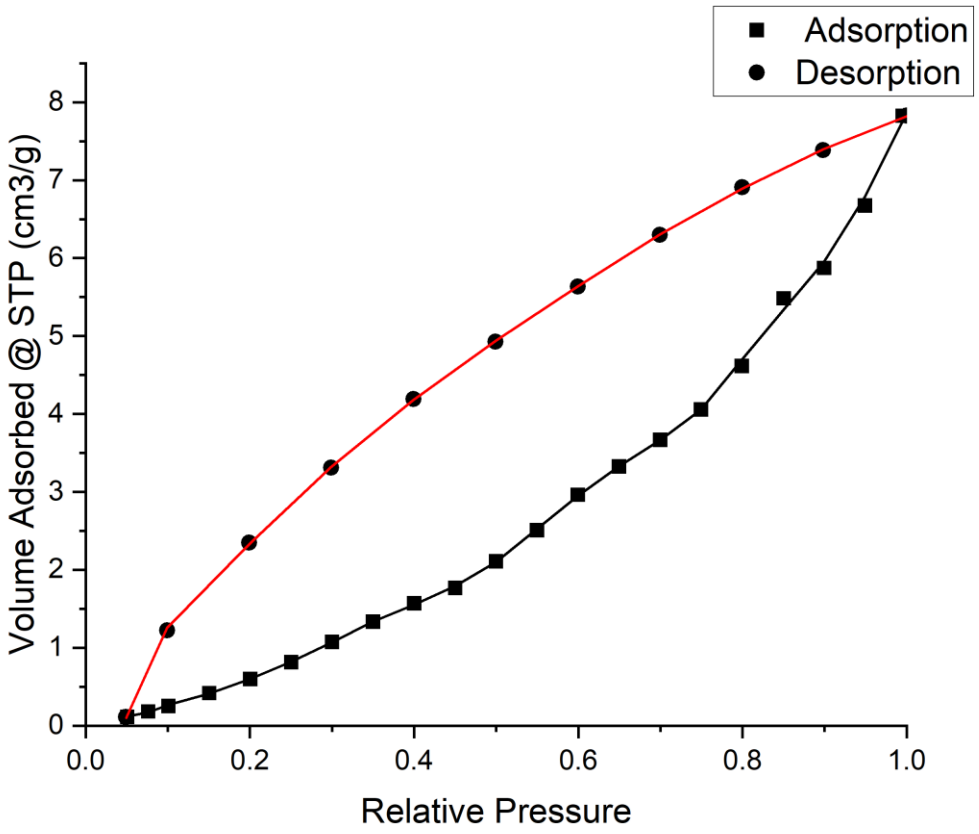


Figure 28: S4 BET isotherm

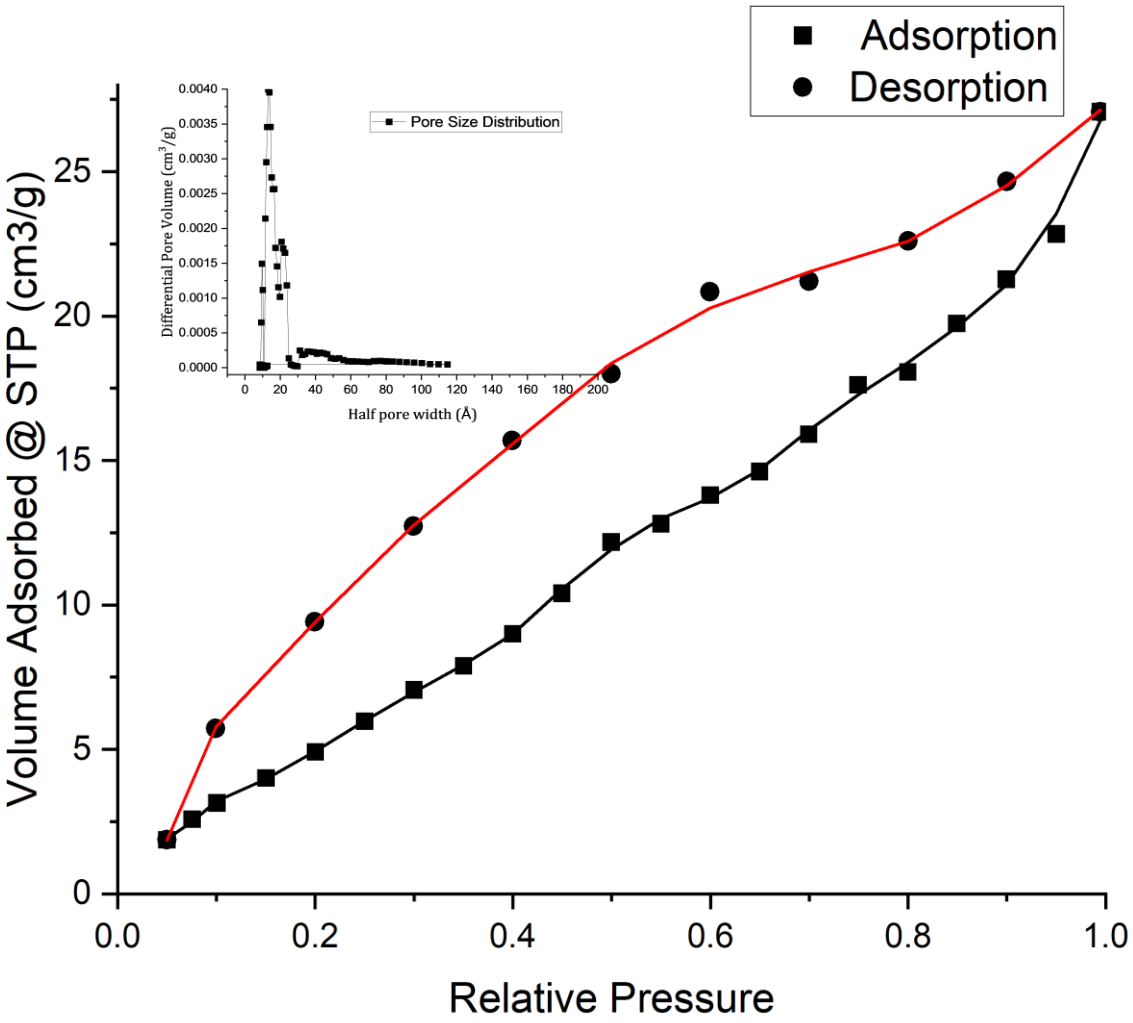


Figure 29: S6 BET isotherm

6.9.TGA analysis

The temperature ranges from 30°C to 150°C represents the loss of adsorbed water or low molecular weight solvents. From the 150°C to 300°C temp range which typically associated with cellulose and other hydroxyl-containing groups, this range can indicate the decomposition of lignocellulosic materials like CNCs. Ester bond (-COO-) present in CNC polymer chain break down in the range of 200°C to 350°C.The temperature Range from 300°C to 500°C is where backbone decomposition of polymers like PEI begins, leading to fragmentation of the molecular structure. Decomposition of aromatic groups, often present in high-temperature stable polymers like PEI occurs in the range 450°C to 600°C, which proves that PEI was properly grafted in the CNC network.

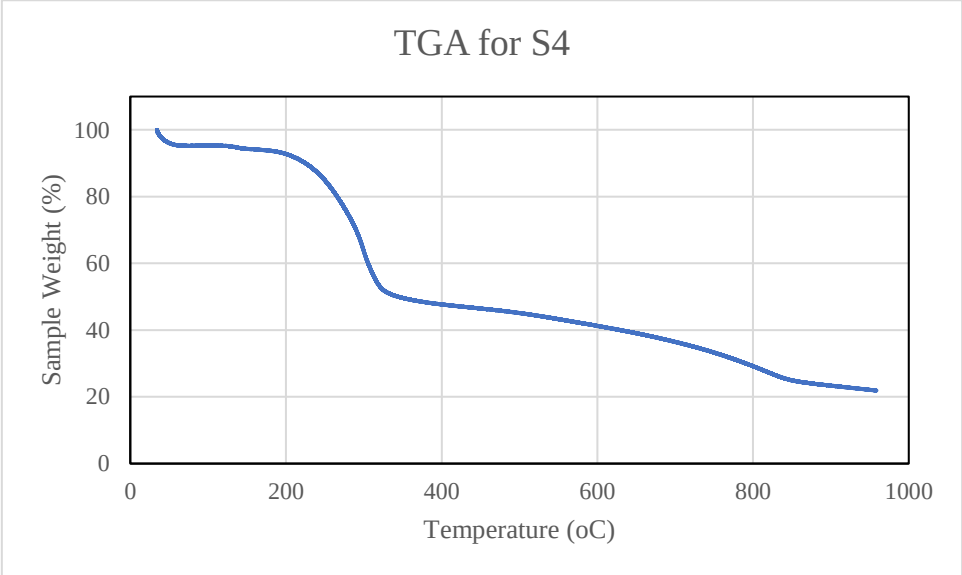


Figure 30: S4 TGA

7. Conclusion

CNC based aerogels have been prepared and fabricated with various cross-linking and binding agents as depicted in Table 4 of 3.2. The functionally modified aerogels were classified and selected based on the surface functional groups and to enhance the adsorption capacity of the selective metal ions, the aerogels were subjected to various parametric changes (e.g., pH, Dosage, Conc, Time). These experiments have provided various insights. Characterizations of the samples were done to understand the adsorption behavior, the surface morphology as well as its structural and thermal stability. This study successfully fabricated CNC based aerogel and evaluated their adsorption capacity towards selective metal ions. The key findings of this research may be summarized as follows:

- **Synthesis parameters**
  The w/v % ratio and chemical concentrations used during these experiments had a major effect on the Aerogel structural stability and adsorption capacity. Addition of PVA in sample S3, S5 and S6 has shown better mechanical stability. The optimum CNC:PVA ratio was found to be 2:1. In case of samples with $NaIO_4$ had provided with better resistance towards degradation. Out of all the samples S6 has shown overall best adsorption capacity for both Cu (II) and Cr (VI) ion in pH 6. It can be inferred that the -CHO and the -NH_2 groups present in the sample had provided better adsorption site for both the ions.
- **Effect of pH and catalyst loading**
  The initial pH of the copper solution has a critical effect on the absorbent adsorption performance as it determines the form of copper ion species as well as the electrostatic repulsive forces between the absorbents and Cu (II) ions. For example, Cu (II) ions transformed to Cu (OH)2 when the pH exceeded 6. At low pH due to the strong electrostatic repulsive force between positively charged PEI and Cu2+ ions. PEI became protonated at pH less than 6, and the protonation degree increased inversely proportional to the pH, hence a suitable pH range of between 6 and 7 should be selected to conduct the adsorption studies. As for the pH, the sustained increased from 7 to 10 suggested that the adsorption was not dominated by H^+ exchange, but rather by the coordination/ chelation between the amine groups and Cu (II) ions.
  In the Cr (VI) removal process, Cr (VI) exists in various oxidation states depending on the solution pH. At pH 2–6, $HCrO_4^{2-}$and $Cr_2O^{2-}_7$ are the most common form, while $HCrO_4^{2-}$is the dominant species when pH>6, and H_2CrO_4 dominates at lower pH. In this experiment at pH 6,S6 has given highest adsorption result for Chromium ion.
- **Characterizations**
  The chemical structure changes of all the samples were investigated by FTIR spectra. Figure 12 shows that the absorption peaks at 3334, 2920, 1160, and 897 cm−1, attributed to the typical features of cellulose, can be observed on both CNCs and, respectively. In addition, the modified has absorption peaks at 2835, and 1446 cm−1, which are attributed to PEI-NH_2 and C-N vibration The increased peak intensity at 1653 cm^{-1} is corresponded to the stretching of C=N group formed in the glutaraldehyde crosslinking process in case of sample 1. These results demonstrated that PEI was successfully introduced into the CNC skeleton.

- **Kinetic studies**

The effects of contact time on Cr (VI) adsorption capacity at different initial concentrations are shown in Figure 15. The uptake capacity rate of S4 increased rapidly in the initial stage and reached above 75% within 180 min due to the numerous active adsorption sites on the surface. Then, with the saturation of adsorption sites, the adsorption rate decreased until the adsorption equilibrium was reached. In addition, with the initial Cr (VI) concentration increase from 10to 1000mg/L, equilibrium adsorption capacity of Cr (VI) also increased while the equilibrium time remained constant. The Cr (VI) adsorption kinetic were correlated using pseudo-1st- and pseudo-2nd-order models, and the relevant kinetic parameters from both models were summarized in Table 5 Compared with pseudo-1st-order, the pseudo-2nd-order kinetic model presents lower R^2 values at different initial Cr (VI) concentrations, indicating that Cr (VI) adsorption process conformed to the pseudo-first-order model well, and was controlled by the electrostatic attraction and diffusive adsorption process.

- **Adsorption studies**

Adsorption isotherm analyses were carried out to examine the adsorption capacity and interactive behaviors between the adsorbent and Cu (II) and Cr (VI) ions. Data shows that the equilibrium adsorption capacity increased rapidly at low Cu (II) ions concentration then slowly increased. the adsorption data, indicating the adsorption sites were homogeneously distributed in the aerogels and the adsorption was monolayer.

8. REFERENCE:

[1] S. Alwin and X. Sahaya Shajan, "Aerogels: promising nanostructured materials for energy conversion and storage applications," Jul. 01, 2020, *Springer Science and Business Media Deutschland GmbH*. doi: 10.1007/s40243-020-00168-4.

[2] R. Fu *et al.*, "The fabrication and characterization of carbon aerogels by gelation and supercritical drying in isopropanol," *Adv Funct Mater*, vol. 13, no. 7, pp. 558–562, Jul. 2003, doi: 10.1002/adfm.200304289.

[3] W. K. Pui, R. Yusoff, and M. K. Aroua, "A review on activated carbon adsorption for volatile organic compounds (VOCs)," Jul. 01, 2019, *De Gruyter*. doi: 10.1515/revce-2017-0057.

[4] L. Yan, H. Ren, J. Zhu, Y. Bi, and L. Zhang, "One-step eco-friendly fabrication of classically monolithic silica aerogels via water solvent system and ambient pressure drying," *Journal of Porous Materials*, vol. 26, no. 3, pp. 785–791, Jun. 2019, doi: 10.1007/s10934-018-0674-4.

[5] P. Shajesh, S. Smitha, P. R. Aravind, and K. G. K. Warrier, "Effect of 3-glycidoxypropyltrimethoxysilane precursor on the properties of ambient pressure dried silica aerogels," *J Solgel Sci Technol*, vol. 50, no. 3, pp. 353–358, Jun. 2009, doi: 10.1007/s10971-009-1926-1.

[6] İ. Şahin, Y. Özbakır, Z. İnönü, Z. Ulker, and C. Erkey, "Kinetics of supercritical drying of gels," Mar. 01, 2018, *MDPI AG*. doi: 10.3390/gels4010003.

[7] H. Maleki and N. Hüsing, "Current status, opportunities and challenges in catalytic and photocatalytic applications of aerogels: Environmental protection aspects," 2018, *Elsevier B.V.* doi: 10.1016/j.apcatb.2017.08.012.

[8] C. A. García-González, M. C. Camino-Rey, M. Alnaief, C. Zetzl, and I. Smirnova, "Supercritical drying of aerogels using CO 2: Effect of extraction time on the end material textural properties," *Journal of Supercritical Fluids*, vol. 66, pp. 297–306, Jun. 2012, doi: 10.1016/j.supflu.2012.02.026.

[9] R. Rodríguez-Dorado, C. López-Iglesias, C. A. García-González, G. Auriemma, R. P. Aquino, and P. Del Gaudio, "Design of aerogels, cryogels and xerogels of alginate: Effect of molecular weight, gelation conditions and drying method on particles' micromeritics," *Molecules*, vol. 24, no. 6, Mar. 2019, doi: 10.3390/molecules24061049.

[10] K. R. Parmar, D. T. K. Dora, K. K. Pant, and S. Roy, "An ultra-light flexible aerogel-based on methane derived CNTs as a reinforcing agent in silica-CMC matrix for efficient oil adsorption," *J Hazard Mater*, vol. 375, pp. 206–215, Aug. 2019, doi: 10.1016/j.jhazmat.2019.04.017.

[11] G. Kumar, D. T. K. Dora, D. Jadav, A. Naudiyal, A. Singh, and T. Roy, "Utilization and regeneration of waste sugarcane bagasse as a novel robust aerogel as an effective thermal, acoustic insulator, and oil adsorbent," *J Clean Prod*, vol. 298, May 2021, doi: 10.1016/j.jclepro.2021.126744.

[12] Y. Chen, Z. Nie, J. Gao, J. Wang, and M. Cai, "A novel adsorbent of bentonite modified chitosan-microcrystalline cellulose aerogel prepared by bidirectional regeneration strategy for Pb(II) removal," *J Environ Chem Eng*, vol. 9, no. 4, Aug. 2021, doi: 10.1016/j.jece.2021.105755.

[13] C. Simón-Herrero, S. Caminero-Huertas, A. Romero, J. L. Valverde, and L. Sánchez-Silva, "Effects of freeze-drying conditions on aerogel properties," *J Mater Sci*, vol. 51, no. 19, pp. 8977–8985, Oct. 2016, doi: 10.1007/s10853-016-0148-5.

[14] F. J. Burpo, E. A. Nagelli, L. A. Morris, J. P. McClure, M. Y. Ryu, and J. L. Palmer, "Direct solution-based reduction synthesis of Au, Pd, and Pt aerogels," *J Mater Res*, vol. 32, no. 22, pp. 4153–4165, Nov. 2017, doi: 10.1557/jmr.2017.412.

[15] R. Muthuraj, Y. Grohens, and B. Seantier, "Mechanical and thermal insulation properties of elium acrylic resin/cellulose nanofiber based composite aerogels," *Nano-Structures and Nano-Objects*, vol. 12, pp. 68–76, Oct. 2017, doi: 10.1016/j.nanoso.2017.09.002.

[16] S. W. Chook *et al.*, "A porous aerogel nanocomposite of silver nanoparticles-functionalized cellulose nanofibrils for SERS detection and catalytic degradation of rhodamine B," *RSC Adv*, vol. 5, no. 108, pp. 88915–88920, 2015, doi: 10.1039/c5ra18806g.

[17] Y. Wang, Y. Li, Y. Zhang, Z. Zhang, Y. Li, and W. Li, "Nanocellulose aerogel for highly efficient adsorption of uranium (VI) from aqueous solution," *Carbohydr Polym*, vol. 267, Sep. 2021, doi: 10.1016/j.carbpol.2021.118233.

[18] F. Placin, J. P. Desvergne, and F. Cansell, "Organic low molecular weight aerogel formed in supercritical fluids," *J Mater Chem*, vol. 10, no. 9, pp. 2147–2149, 2000, doi: 10.1039/b001714k.

[19] "irina gurikov".

[20] S. Dolai, S. K. Bhunia, and R. Jelinek, "Carbon-dot-aerogel sensor for aromatic volatile organic compounds," *Sens Actuators B Chem*, vol. 241, pp. 607–613, Mar. 2017, doi: 10.1016/j.snb.2016.10.124.

[21] "gurikov".

[22] J. Fan *et al.*, "Substantial convection and precipitation enhancements by ultrafine aerosol particles," *Science (1979)*, vol. 359, no. 6374, pp. 411–418, Jan. 2018, doi: 10.1126/science.aan8461.

[23] J. Yin *et al.*, "Bioinspired and dual-functional nanocellulose aerogels for water disinfection and heavy metal removal," *Nano Today*, vol. 51, Aug. 2023, doi: 10.1016/j.nantod.2023.101918.

[24] J. Zhao *et al.*, "Self-cross-linking of metal-organic framework (MOF-801) in nanocellulose aerogel for efficient adsorption of Cr (VI) in water," *Sep Purif Technol*, vol. 327, Dec. 2023, doi: 10.1016/j.seppur.2023.124942.

[25] L. Fu and C. Hou, "A polydiacetylene-based smart cellulose aerogel functionalized by ZnO/MoS2 heterojunction for simultaneous visual detection and photocatalytic degradation of gaseous VOCs," *Sep Purif Technol*, vol. 314, Jun. 2023, doi: 10.1016/j.seppur.2023.123512.

[26] N. G. Camparotto, T. de F. Neves, V. R. Mastelaro, and P. Prediger, "Hydrophobization of aerogels based on chitosan, nanocellulose and tannic acid: Improvements on the aerogel features and the adsorption of contaminants in water," *Environ Res*, vol. 220, Mar. 2023, doi: 10.1016/j.envres.2022.115197.

[27] Z. Hu, J. Yang, M. Liu, W. Rao, Y. Xie, and C. Yu, "Amine-functionalized cellulose nanofiber-sodium alginate-Fe(III) porous hollow beads for the efficient removal of Cr(VI)," *Cellulose*, vol. 30, no. 6, pp. 3807–3822, Apr. 2023, doi: 10.1007/s10570-023-05123-w.

[28] R. Li *et al.*, “Lignosulfonate-Based Hybrid Hydrogels Functionalized with Hyperbranched Polyamide Amine as Ultra-High-Capacity Adsorbent for Congo Red Removal from Aqueous Solutions,” *Water Air Soil Pollut*, vol. 234, no. 3, Mar. 2023, doi: 10.1007/s11270-023-06162-6.

[29] D. F. Alves, P. H. Camani, A. G. Souza, and D. S. Rosa, “A novel sustainable composite hydrogel containing nanocellulose to remove potentially toxic metals from contaminated water,” *Polymer Bulletin*, 2023, doi: 10.1007/s00289-023-04986-0.

[30] C. Qiu, Y. Li, H. Liu, X. Wang, S. Hu, and H. Qi, “A novel crosslinking strategy on functional cellulose-based aerogel for effective and selective removal of dye,” *Chemical Engineering Journal*, vol. 463, May 2023, doi: 10.1016/j.cej.2023.142404.

[31] H. Li *et al.*, “Hierarchically porous poly(amidoxime)/bacterial cellulose composite aerogel for highly efficient scavenging of heavy metals,” *J Colloid Interface Sci*, vol. 600, pp. 752–763, Oct. 2021, doi: 10.1016/j.jcis.2021.05.071.

[32] Y. Chen, Z. Nie, J. Gao, J. Wang, and M. Cai, “A novel adsorbent of bentonite modified chitosan-microcrystalline cellulose aerogel prepared by bidirectional regeneration strategy for Pb(II) removal,” *J Environ Chem Eng*, vol. 9, no. 4, Aug. 2021, doi: 10.1016/j.jece.2021.105755.

[33] Y. Lv *et al.*, “Efficient adsorption of diclofenac sodium in water by a novel functionalized cellulose aerogel,” *Environ Res*, vol. 194, Mar. 2021, doi: 10.1016/j.envres.2020.110652.

[34] H. Khawaja, E. Zahir, M. A. Asghar, and M. A. Asghar, “Graphene oxide decorated with cellulose and copper nanoparticle as an efficient adsorbent for the removal of malachite green,” *Int J Biol Macromol*, vol. 167, pp. 23–34, Jan. 2021, doi: 10.1016/j.ijbiomac.2020.11.137.

[35] C. Peng *et al.*, “A novel cellulose nanocrystal-based antifungal aerogel for fluorometric detection and efficient removal of Cr(VI),” *Ind Crops Prod*, vol. 189, Dec. 2022, doi: 10.1016/j.indcrop.2022.115743.

[36] V. T. Nguyen, L. Q. Ha, T. D. L. Nguyen, P. H. Ly, D. M. Nguyen, and D. Hoang, “Nanocellulose and Graphene Oxide Aerogels for Adsorption and Removal Methylene Blue from an Aqueous Environment,” *ACS Omega*, vol. 7, no. 1, pp. 1003–1013, Jan. 2022, doi: 10.1021/acsomega.1c05586.

[37] H. J. Hong, G. Ban, H. S. Kim, H. S. Jeong, and M. S. Park, “Fabrication of cylindrical 3D cellulose nanofibril(CNF) aerogel for continuous removal of copper(Cu2+) from wastewater,” *Chemosphere*, vol. 278, Sep. 2021, doi: 10.1016/j.chemosphere.2021.130288.

[38] L. Liang, S. Zhang, G. A. Goenaga, X. Meng, T. A. Zawodzinski, and A. J. Ragauskas, “Chemically Cross-Linked Cellulose Nanocrystal Aerogels for Effective Removal of Cation Dye,” *Front Chem*, vol. 8, Jul. 2020, doi: 10.3389/fchem.2020.00570.

[39] R. E. Abou-Zeid, K. A. Ali, R. M. A. Gawad, K. H. Kamal, S. Kamel, and R. Khiari, “Removal of cu(Ii), pb(ii), mg(ii), and fe(ii) by adsorption onto alginate/nanocellulose beads as bio-sorbent,” *J Renew Mater*, vol. 9, no. 4, pp. 601–613, 2021, doi: 10.32604/jrm.2021.014005.